

# Targeting PI3K $\gamma$ activity decreases vascular trauma-induced intimal hyperplasia through modulation of the Th1 response

Natalia F. Smirnova,<sup>1,2</sup> Stéphanie Gayral,<sup>1,2</sup> Christophe Pedros,<sup>3,4,5</sup>  
Gervaise Loirand,<sup>6,7</sup> Nathalie Vaillant,<sup>6,7</sup> Nicole Malet,<sup>1,2</sup> Sahar Kassem,<sup>3,4,5</sup>  
Denis Calise,<sup>1,2</sup> Dominique Goudounèche,<sup>2,8</sup> Matthias P. Wymann,<sup>9</sup>  
Emilio Hirsch,<sup>10</sup> Alain-Pierre Gadeau,<sup>11</sup> Laurent O. Martinez,<sup>1,2</sup>  
Abdelhadi Saoudi,<sup>3,4,5</sup> and Muriel Laffargue<sup>1,2</sup>

<sup>1</sup>INSERM, UMR1048, F-31300 Toulouse, France

<sup>2</sup>Université Toulouse III, Institut de Maladies Métaboliques et Cardiovasculaires, F-31300 Toulouse, France

<sup>3</sup>INSERM, UMR1043, F-31300 Toulouse, France

<sup>4</sup>UMR CNRS, U5282, F-31300 Toulouse, France

<sup>5</sup>Université de Toulouse, UPS, Centre de Physiopathologie de Toulouse Purpan (CPTP), F-31300 Toulouse, France

<sup>6</sup>INSERM, UMR1087, F-44007 Nantes, France

<sup>7</sup>CNRS 6291, F-44007 Nantes, France

<sup>8</sup>CMEAB, F-31000 Toulouse, France

<sup>9</sup>Institute of Biochemistry and Genetics, University of Basel, 4058 Basel, Switzerland

<sup>10</sup>Molecular Biotechnology Center, Department of Molecular Biotechnology and Health Sciences, University of Turin, 10124 Turin, Italy

<sup>11</sup>INSERM U1034, F-33600 Pessac, France

**Interventional strategies to treat atherosclerosis, such as transluminal angioplasty and stent implantation, often cause vascular injury. This leads to intimal hyperplasia (IH) formation that induces inflammatory and fibroproliferative processes and ultimately restenosis. We show that phosphoinositide 3-kinase  $\gamma$  (PI3K $\gamma$ ) is a key player in IH formation and is a valid therapeutic target in its prevention/treatment. PI3K $\gamma$ -deficient mice and mice expressing catalytically inactive PI3K $\gamma$  (PI3K $\gamma$  KD) showed reduced arterial occlusion and accumulation of monocytes and T cells around sites of vascular lesion. The transfer of PI3K $\gamma$  KD CD4<sup>+</sup> T cells into Rag2-deficient mice greatly reduced vascular occlusion compared with WT cells, clearly demonstrating the involvement of PI3K $\gamma$  in CD4<sup>+</sup> T cells during IH formation. In addition we found that IH is associated with increased levels of Th1 and Th17 cytokines. A specific decrease in the Th1 response was observed in the absence of PI3K $\gamma$  activity, leading to decreased CXCL10 and RANTES production by smooth muscle cells. Finally, we show that treatment with the PI3K $\gamma$  inhibitor AS-605240 is sufficient to decrease IH in both mouse and rat models, reinforcing the therapeutic potential of PI3K $\gamma$  inhibition. Altogether, these findings demonstrate a new role for PI3K $\gamma$  activity in Th1-controlled IH development.**

## CORRESPONDENCE

M. Laffargue:  
muriel.laffargue@inserm.fr  
OR

S. Gayral:  
stephanie.gayral@inserm.fr.

Abbreviations used: DES, drug-eluting stent; IH, intimal hyperplasia; ILN, inguinal LN; PI3K $\gamma$ , phosphoinositide 3-kinase  $\gamma$ ; SMC, smooth muscle cell.

Vascular disease is a significant cause of morbidity and mortality in developed countries and results from vascular injury. Among pathological phenomena that take place in the arterial wall, intimal hyperplasia (IH) usually precedes atherosclerosis and is a complication of transluminal angioplasty and stent implantation which are interventional strategies used in the treatment of atherosclerosis (Bennett, 2003). IH is an exaggerated healing process of the vessel wall defined as the formation of a multicellular layer within the arterial lumen and characterized by

inflammatory and fibroproliferative responses. Injury of the endothelium leads to the recruitment of activated platelets and leukocytes (Costa and Simon, 2005), followed by abnormal proliferation and migration of medial smooth muscle cells (SMCs) that subsequently undergo a dedifferentiation process. This results in fibrocellular intimal thickening and a reduction in blood flow,

© 2014 Smirnova et al. This article is distributed under the terms of an Attribution-Noncommercial-Share Alike-No Mirror Sites license for the first six months after the publication date (see <http://www.rupress.org/terms>). After six months it is available under a Creative Commons License (Attribution-Noncommercial-Share Alike 3.0 Unported license, as described at <http://creativecommons.org/licenses/by-nc-sa/3.0/>).

**Table 1.** Morphometric analysis of injured WT, PI3K $\gamma$  KD, and PI3K $\gamma$  KO femoral arteries

Mice	Intima	Media	Lumen	IEL	EEL
	$\mu m^2$	$\mu m^2$	$\mu m^2$	$\mu m^2$	$\mu m^2$
WT	26,020 $\pm$ 3,313	11,880 $\pm$ 1,344	12,100 $\pm$ 1,118	38,120 $\pm$ 3,713	49,990 $\pm$ 4,781
PI3K $\gamma$ KD	10,580 $\pm$ 2,988** P = 0.0011	14,340 $\pm$ 1,384 P = 0.1138	22,250 $\pm$ 4,217* P = 0.0378	32,830 $\pm$ 3,737 P = 0.5981	47,170 $\pm$ 4,781 P = 0.8768
PI3K $\gamma$ KO	7,850 $\pm$ 1,605*** P < 0.0001	14,300 $\pm$ 1,024 P = 0.0578	24,570 $\pm$ 3,564* P = 0.0103	32,420 $\pm$ 3,144 P = 0.5050	46,720 $\pm$ 3,882 P = 0.9591

Femoral arteries from WT ( $n = 13$ ), PI3K $\gamma$  KD ( $n = 9$ ), and PI3K $\gamma$  KO mice ( $n = 11$ ) were mechanically injured and analyzed 28 d after injury. IEL and EEL, respectively, indicate areas defined by the internal elastic laminae and external elastic laminae. Data are expressed as mean  $\pm$  SEM for each group and are representative of two independent experiments,  $n = 9$ –13 mice per group. \*,  $P < 0.05$ ; \*\*,  $P < 0.01$ ; \*\*\*,  $P < 0.001$  versus WT controls. Data were analyzed with a Mann-Whitney test.

which can have dramatic consequences especially if a coronary artery is affected.

Many studies have focused on the proliferative component of IH as the target for treatment (Lindner et al., 1993; Schwartz et al., 1998; Dzau, 2003). Drug-eluting stents (DESs) coated with antiproliferative agents have been shown to have beneficial effects on the development of IH (Bikkina and Koneru, 2011); however, the lack of specificity of the DES is thought to cause side effects such as thrombosis (Lagerqvist et al., 2007). Moreover, some patients have presented with genetic resistance to either the eluted drugs or the polymer used to recover the stent (Dangas et al., 2010). These issues highlight the urgent need to identify new therapeutic targets for IH.

Recently, inflammation has emerged as a key process at the heart of IH development, revealing a whole new array of possible targets for the control of neointimal formation. Various studies have shown an association between in-stent restenosis and inflammation in patients. For example, the fracture of a metallic stent placed in the femoral artery was shown to correlate with both a greater recruitment of inflammatory cells around the stent and a subsequent increase in the severity of restenosis (Farb et al., 2002). In response to injury, leukocytes are recruited to the arterial wall (Boehm et al., 2004; Marx et al., 2011) and an acute inflammatory response has been shown to initiate the development of IH. In agreement with this, intimal thickening can be reduced by inhibition of leukocyte recruitment through modulation of the MCP-1–CCR2 signaling pathway in animal models of arterial injury (Horvath et al., 2002; Grassia et al., 2009). The sequence of events immediately after arterial injury has recently been characterized and involves the recruitment of inflammatory cells and the expression of proinflammatory cytokines (Kovacic et al., 2010); the subsequent increase in the concentrations of growth factors and cytokines then activates SMC to migrate and proliferate (Marx et al., 2011). Therefore, modulating the acute immune response may be an alternative strategy to inhibit IH, thus avoiding the nonspecific side effects of anti-proliferative agents.

In this context, class IB phosphoinositide 3-kinase  $\gamma$  (PI3K $\gamma$ ) is of particular interest in the study of inflammatory and cardiovascular pathologies. PI3K $\gamma$  is largely expressed in inflammatory cells but has also been identified in cells of the cardiovascular

system, particularly endothelial cells and SMC. The recruitment of this kinase downstream of G protein–coupled receptors accounts for its implication in the chemotactic migration of leukocytes because these receptors are largely responsible for binding chemokines and directing cell migration in leukocytes. PI3K $\gamma$ -deficient mice (PI3K $\gamma$  KO) have been used to demonstrate that PI3K $\gamma$  is involved in numerous biological functions of immune cells such as monocyte/macrophage recruitment to inflammatory sites (Hirsch et al., 2000), thymocyte development (Sasaki et al., 2000), T lymphocyte activation (Alcázar et al., 2007), and mastocyte degranulation (Laffargue et al., 2002). In arterial studies, both treatment with a specific PI3K $\gamma$  inhibitor and the specific deletion of PI3K $\gamma$  in the immune system in LDLR $^{-/-}$  mice reduced atherosclerotic lesions by preventing inflammatory processes occurring in the vascular wall (Fougerat et al., 2008). Moreover, the generation of a mouse model expressing a catalytically inactive form of PI3K $\gamma$  (PI3K $\gamma$  kinase dead, KD) allowed the analysis of PI3K-dependent from PI3K-independent functions in cardiac cells (Patrucco et al., 2004; Perino et al., 2011). This useful model mimics the effects of a pharmacological inhibitor of the kinase while preserving any eventual off-target side effects. Finally, PI3K $\gamma$  has recently been identified as a mediator of vascular SMC migration (Fougerat et al., 2012). Together, these studies suggest that PI3K $\gamma$  could play an important role in the development of IH.

Here, using genetic and pharmacological approaches, we have identified PI3K $\gamma$  as an essential mediator of acute inflammatory vascular events during neointima formation. Lymphocyte-deficient mice and BM chimeras were used to demonstrate that, after vascular injury, the activity of PI3K $\gamma$  clearly controls CD4 $^{+}$  T cell–induced IH. We found that Th1 and Th17 cytokines were produced during IH progression and that the absence of PI3K $\gamma$  activity specifically modulated the Th1 cytokine profile, which had an impact on the SMC inflammatory response. Finally, we show that a short period of treatment with a PI3K $\gamma$  inhibitor decreased IH development in two different but complementary animal models: a mouse femoral artery mechanical injury model and a rat carotid artery balloon injury model. These data open the perspective of investigating PI3K $\gamma$  as a target for the prevention of arterial damage in interventional cardiology.

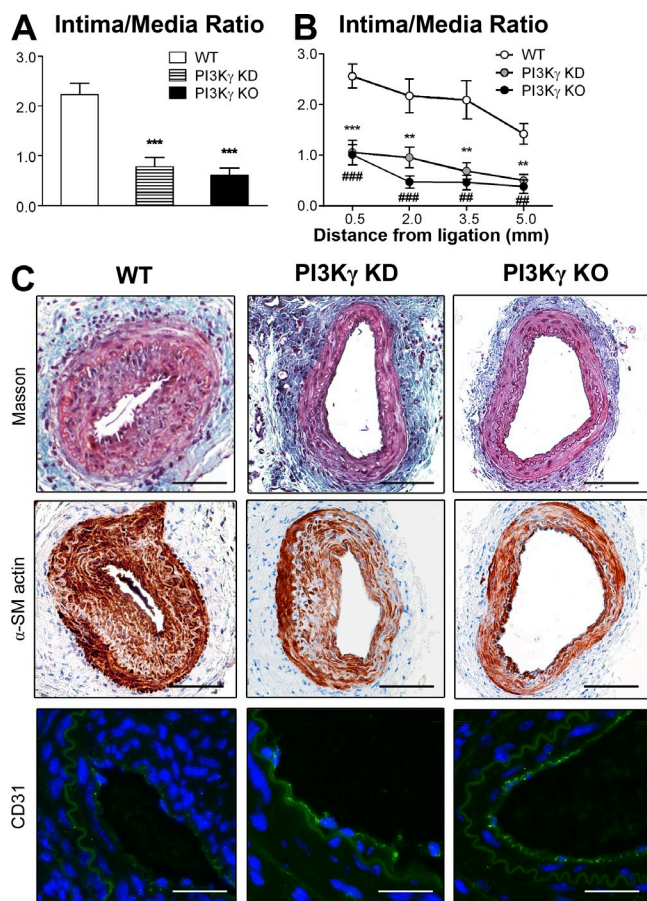


**Figure 1. Lack of PI3K $\gamma$  activity leads to a dramatic decrease in IH.** Femoral arteries from WT, PI3K $\gamma$  KD, and PI3K $\gamma$  KO mice were mechanically injured and analyzed 28 d after injury. (A) Histogram shows quantitative analysis of the intima/media ratio in indicated mice. (B) Graph shows the intima/media ratio at each distance from ligation of the injured femoral arteries. (C) Representative cross sections of femoral injured arteries stained with Masson Trichrome (top), immunostained for  $\alpha$ -smooth muscle ( $\alpha$ -SM) actin (middle), or immunostained for CD31 (green) and DAPI for nuclear staining (bottom). Bars: (Masson Trichrome and  $\alpha$ -SM actin) 100  $\mu$ m; (CD31) 50  $\mu$ m. Data are expressed as mean  $\pm$  SEM and are representative of two independent experiments.  $n = 9$ –13 mice per group. A: \*\*\*,  $P < 0.001$ . B: \*\*,  $P < 0.01$  (PI3K $\gamma$  KD vs. WT); \*\*\*,  $P < 0.001$  (PI3K $\gamma$  KD vs. WT); \*\*,  $P < 0.01$  (PI3K $\gamma$  KO vs. WT); \*\*\*,  $P < 0.001$  (PI3K $\gamma$  KO vs. WT). Data were analyzed with a Mann-Whitney test.

## RESULTS

### Genetic targeting of PI3K $\gamma$ activity leads to decreased neointimal formation after vascular injury

To investigate the functional role of PI3K $\gamma$  in response to arterial injury, we induced a mechanical injury of the femoral artery in WT, PI3K $\gamma$  KD, and PI3K $\gamma$  KO mice and analyzed neointimal formation 28 d later. Morphometric analysis of injured femoral arteries showed a significant decrease in intimal area, accompanied by a significant increase in lumen area in PI3K $\gamma$  KD and PI3K $\gamma$  KO mice compared with WT controls (Table 1). Normalization with the medial area showed that the mean intima/media ratio in PI3K $\gamma$  KD and PI3K $\gamma$

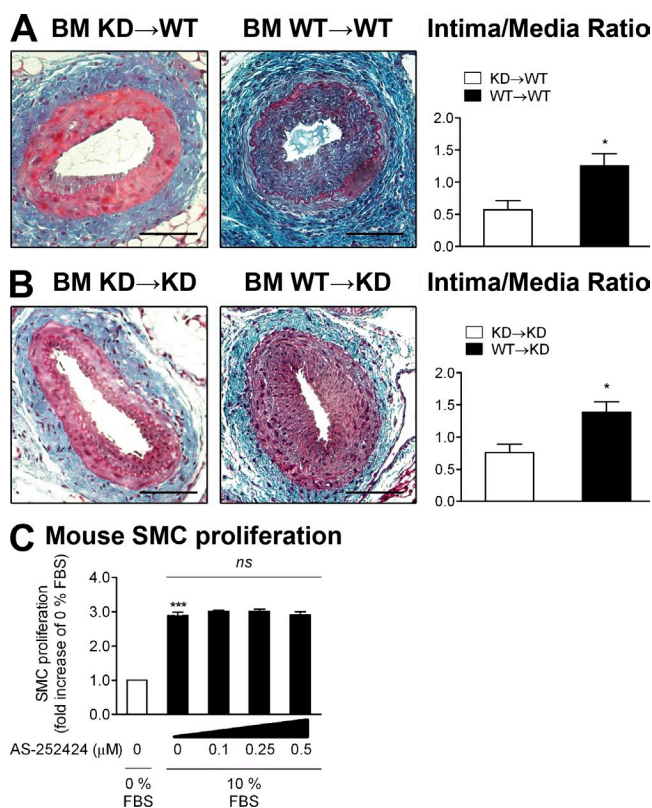


**Figure 2. Immune PI3K $\gamma$  activity is involved in IH.** (A) Irradiated WT mouse recipients were transplanted with BM from PI3K $\gamma$  KD or WT donors to obtain hematopoietic chimeras (BM KD $\rightarrow$ WT and BM WT $\rightarrow$ WT). 4 wk later, mice were mechanically injured and analyzed 28 d after injury. Left: representative cross sections of injured femoral arteries stained with Masson Trichrome. Right: quantitative analysis of intima/media ratios of indicated hematopoietic chimeras. (B) Irradiated PI3K $\gamma$  KD mouse recipients were transplanted with BM from PI3K $\gamma$  KD or WT donors to obtain hematopoietic chimeras (BM KD $\rightarrow$ KD and BM WT $\rightarrow$ KD). 4 wk later, mice were mechanically injured and analyzed 28 d after injury. Left: representative sections of injured femoral arteries stained with Masson Trichrome. Right: quantitative analysis of intima/media ratios of indicated hematopoietic chimeras. (C) Mouse primary SMC proliferation was evaluated in 0 or 10% FBS. The effect of a dose-response of the PI3K $\gamma$  selective inhibitor AS-252424 was assessed under 10% FBS conditions. Proliferation rate is expressed as fold increase over the 0% FBS condition. Bars, 100  $\mu$ m. Data are expressed as mean  $\pm$  SEM and are representative of two independent experiments for A and B, and of three independent experiments for C.  $n = 6$ –10 mice per group. \*,  $P < 0.05$ ; \*\*\*,  $P < 0.001$ ; ns, nonsignificant. Data were analyzed with a Mann-Whitney test.

KO mice was reduced by 72 and 76%, respectively, compared with WT mice (intima/media ratios: WT,  $2.37 \pm 0.29$  vs. PI3K $\gamma$  KD,  $0.67 \pm 0.16$ ,  $P = 0.0002$ ; WT vs. PI3K $\gamma$  KO,  $0.58 \pm 0.12$ ,  $P < 0.0001$ ; Fig. 1 A). For all groups the intima/media ratio was calculated from the same vessel segment to avoid neointimal variability in the distance from the ligation point. At each distance, the intima/media ratio was significantly lower in PI3K $\gamma$  KD and PI3K $\gamma$  KO mice compared with WT controls (Fig. 1 B). Histological analysis of the injured arteries (Fig. 1 C) showed a larger neointima in WT arteries compared



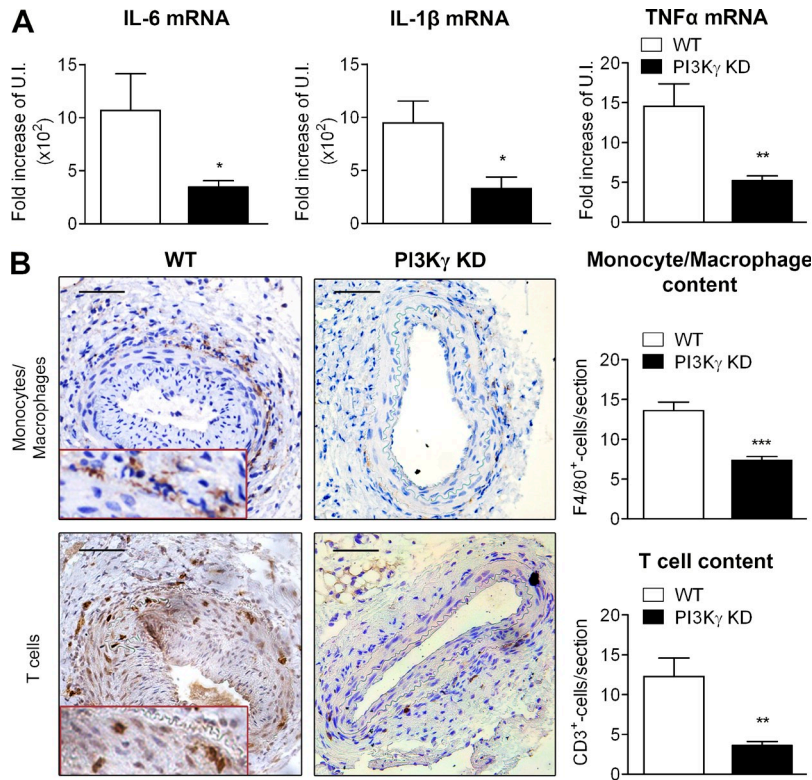


**Figure 3. PI3K $\gamma$  activity is required for sequential infiltration of monocytes and T lymphocytes around the arterial lesion.** (A) Femoral arteries from WT and PI3K $\gamma$  KD were mechanically injured and analyzed 6 h later. Histograms show quantitative PCR analysis of IL-6, IL-1 $\beta$ , and TNF expression in the femoral arteries of indicated mice. (B) Femoral arteries from WT and PI3K $\gamma$  KD mice were mechanically injured and analyzed 28 d after injury. Representative photomicrographs show femoral artery sections and histograms show quantitative analysis of the monocyte/macrophage content after F4/80 staining (top) or T lymphocyte content after CD3 staining (bottom). Bars, 100  $\mu$ m. Data are expressed as mean  $\pm$  SEM of fold increase over uninjured artery (U.I.) for A and as mean  $\pm$  SEM over WT controls for B. Data are representative of two independent experiments.  $n = 5-9$  mice per group. \*,  $P < 0.05$ ; \*\*,  $P < 0.01$ ; \*\*\*,  $P < 0.001$ . Data were analyzed with Mann-Whitney test.

with PI3K $\gamma$  KD and PI3K $\gamma$  KO vessels after Masson Trichrome staining (Fig. 1 C, top). Most neointimal cells expressed  $\alpha$ -smooth muscle actin (Fig. 1 C, middle), suggesting an increased proliferation of SMC within the lesion. Interestingly, anti-CD31 immunostaining of endothelial cells indicated an incomplete endothelial coverage in WT mice, whereas it was more complete in PI3K $\gamma$  KD and PI3K $\gamma$  KO animals (Fig. 1 C, bottom), suggesting that the absence of PI3K $\gamma$  activity had improved endothelial healing in this model. These data demonstrate an important role for PI3K $\gamma$  in the development of IH after mechanical injury of femoral arteries. Moreover, the deletion of the whole enzyme or its catalytic activity shows similar responses, thus suggesting a kinase-dependent effect in the development of IH.

#### PI3K $\gamma$ kinase activity in BM-derived cells is necessary for IH development

PI3K $\gamma$  inhibition has an antiinflammatory effect on atherosclerosis (Fougerat et al., 2008) and the activity of PI3K $\gamma$  is important for SMC migration (Fougerat et al., 2012). We therefore sought to compare the roles of PI3K $\gamma$  activity in immune cells versus nonimmune cells in the development of IH. For this purpose, we generated BM chimera by transplanting BM from PI3K $\gamma$  KD donors into WT recipients and vice versa. Controls were PI3K $\gamma$  KD mice who received PI3K $\gamma$  KD BM (BM KD $\rightarrow$ KD) and WT mice who received WT BM (BM WT $\rightarrow$ WT). 4 wk after BM transplantation, analysis of chimerism showed complete engraftment of donor BM in recipients (unpublished data). After engraftment, the

femoral arteries of chimeric mice were injured, and then lesion sizes were quantified 28 d later. In BM KD $\rightarrow$ WT chimeras, the intima/media ratio was decreased by 52% compared with BM WT $\rightarrow$ WT chimeras (Fig. 2 A), whereas a WT immune system on a PI3K $\gamma$  KD background (BM WT $\rightarrow$ KD) reestablished the IH rate to that of a WT background (Fig. 2 B), demonstrating the importance of immune PI3K $\gamma$  activity in IH. BM KD $\rightarrow$ KD chimeras had a similar intima/media ratio as BM KD $\rightarrow$ WT mice. Moreover, the use of a pharmacological inhibitor of PI3K $\gamma$  in primary vascular SMC, even at high doses, did not impact on SMC proliferation (Fig. 2 C), further ruling out direct effect of PI3K $\gamma$  in SMC during IH. Our data indicate that the absence of catalytically active PI3K $\gamma$  in BM-derived cells alone is sufficient to prevent fibroproliferative mechanism at the same rate as the ubiquitous inactivation of the kinase.

#### PI3K $\gamma$ activity is responsible for early inflammation and the sequential recruitment of monocytes/macrophages and T cells around the lesion site

Given the important functional involvement of PI3K $\gamma$  in the immune system, we then compared the local inflammatory profile in WT and PI3K $\gamma$  KD arteries 6 h after injury. The expression of three main proinflammatory mediators (IL-6, IL-1 $\beta$ , and TNF) was assessed by quantitative PCR. IL-6, IL-1 $\beta$ , and TNF mRNA expression was significantly decreased in the absence of PI3K $\gamma$  activity (Fig. 3 A).

To dissect the cellular mechanisms involved in PI3K $\gamma$ -mediated IH, we characterized the immune cells that had

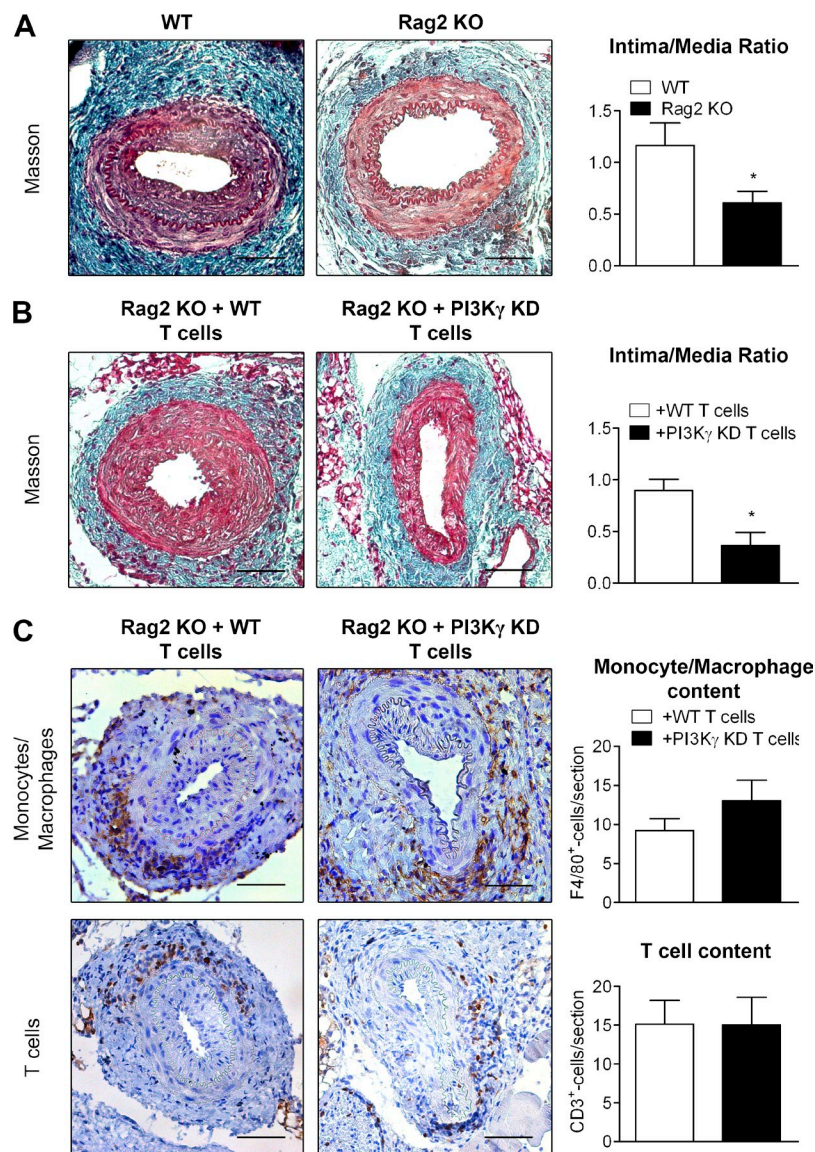


**Figure 4. PI3K $\gamma$  activity in T lymphocytes is involved in IH.** (A) Femoral arteries from WT mice and Rag2 KO mice were mechanically injured and analyzed 28 d after injury. Representative sections show injured femoral arteries stained with Masson Trichrome and histogram shows quantitative analysis of the intima/media ratio of indicated mice. (B and C) Rag2 KO recipient mice were reconstituted with T lymphocytes from WT or PI3K $\gamma$  KD donors (Rag2 KO + WT T cells; Rag2 KO + PI3K $\gamma$  KD T cells). 28 d later, the femoral arteries of mice were mechanically injured and analyzed 28 d after injury. (B) Representative sections show injured femoral arteries stained with Masson Trichrome and histogram shows quantitative analysis of the intima/media ratio of indicated mice. (C) Representative photomicrographs show sections of injured femoral arteries and histograms show quantitative analysis of monocyte/macrophage content after F4/80 staining or T lymphocyte content after CD3 staining. Bars, 100  $\mu$ m. Data are expressed as mean  $\pm$  SEM and are representative of two independent experiments.  $n = 5-15$  mice per group. \*,  $P < 0.05$ . Data were analyzed with Mann-Whitney test.

infiltrated the vessel walls around the injured site in WT mice at different time points after injury. Monocytes/macrophages (F4/80<sup>+</sup> cells) accumulated around the vessels 3 d after the injury, whereas few lymphocytes (CD3<sup>+</sup> cells) were observed (not depicted). At days 8 (not depicted) and 28 (Fig. 3 B), F4/80 staining became less pronounced, whereas CD3-positive cells became more numerous than at day 3. The accumulation of T cells was observed in the periadventitial tissue and in the neointima. Interestingly, PI3K $\gamma$  KD artery sections showed less monocytes/macrophages and a reduction in T cell recruitment around the lesion site compared with WT arteries, suggesting a role for PI3K $\gamma$  in the recruitment of both cell types (Fig. 3 B).

#### PI3K $\gamma$ activity drives CD4<sup>+</sup> T cell-induced IH development

To explore the role played by lymphocytes in the development of IH, we performed arterial injury in Rag2 KO mice that are deficient in mature T and B lymphocytes. Consistent

with previous findings (Boehm et al., 2004), Rag2 KO mice exhibited a 53% lower intima/media ratio compared with WT mice (Fig. 4 A), suggesting that lymphocytes promote IH development. Reconstitution with WT but not PI3K $\gamma$  KD T cells was able to restore IH (Fig. 4 B), demonstrating the central function of PI3K $\gamma$  activity in T cells during IH development. In this Rag2 KO mouse model, monocytes/macrophages with active PI3K $\gamma$  were recruited at the same rate whether reconstituted with WT or PI3K $\gamma$  KD T cells (Fig. 4 C). Interestingly, T cells were also recruited at the same rate around the vessel irrespective of PI3K $\gamma$  activity (Fig. 4 C). These results demonstrate that the specific deletion of PI3K $\gamma$  in T cells is sufficient to prevent IH despite a normal recruitment of immune cells, suggesting a functional role of PI3K $\gamma$  in T cells during IH development. To further characterize the T cell subpopulations involved in these processes, we evaluated the CD4<sup>+</sup> and CD8<sup>+</sup> T cell populations present in injured arteries at day 28 after arterial lesion induction. Results show that the



T cells that had infiltrated the periadventitial tissue were mainly CD4<sup>+</sup>T cells (Fig. 5A), whereas CD8<sup>+</sup> cells were undetectable. In agreement, injection of WT CD4<sup>+</sup> T cells into Rag2 KO mice increased IH compared with Rag2 KO mice that did not receive CD4<sup>+</sup> cells, showing that the CD4<sup>+</sup> subpopulation is involved in the development of this pathology (Fig. 5B). Importantly, PI3K $\gamma$  KD CD4<sup>+</sup> cells failed to increase IH, demonstrating that this kinase plays a key role in the action of CD4<sup>+</sup> cells (Fig. 5B).

#### Specific modulation of the Th1 response in the absence of PI3K $\gamma$ activity reduces the SMC inflammatory response

The cytokine profile of CD4<sup>+</sup> T cells plays a central role in orchestrating the outcome of an immune response. To specifically define which types of cytokine were present in injured femoral arteries, we used an ex vivo system. Injured and uninjured femoral artery rings from WT and PI3K $\gamma$  KD mice were incubated with a PMA/Ionomycin cocktail. After 72 h, the release of IFN- $\gamma$ , IL-4, and IL-17 was measured, classically reflecting the Th1, Th2, and Th17 subpopulations, respectively. Interestingly, IFN- $\gamma$  and IL-17 were detected at high levels in injured arteries, whereas poor levels of IL-4 were produced, indicating that Th1- and Th17-related cytokines are those predominantly involved in IH (Fig. 6A). In addition, in the absence of PI3K $\gamma$  activity, IL-4 and IL-17 levels were not modified, whereas IFN- $\gamma$  levels were dramatically decreased, demonstrating that PI3K $\gamma$  activity specifically modulates Th1 cytokines during IH progression (Fig. 6A). We also analyzed the intracytoplasmic content of IFN- $\gamma$  and IL-17 by CD4<sup>+</sup> T cells collected from inguinal LNs (ILNs) and showed an increase in IFN- $\gamma$  after injury. As we observed in injured arteries, the absence of PI3K $\gamma$  activity led to a dramatic decrease in IFN- $\gamma$ , confirming the importance of PI3K $\gamma$  in the Th1 response (Fig. 6B). Surprisingly, we did not observe any difference concerning the IL-17 production by CD4<sup>+</sup> T cells originating from injured mice compared with uninjured mice. This contrasts with our results in injured arteries and suggests that a population other than CD4<sup>+</sup> T cells is responsible for IL-17 production (not depicted). Interestingly, we also found that CXCL10 and RANTES, both involved in leukocyte recruitment, were secreted at high levels in injured femoral arteries compared with uninjured arteries and that their levels were dramatically lower in the absence of PI3K $\gamma$ , indicating that PI3K $\gamma$  was responsible for their secretion at the site of injury (Fig. 6C).

Based on these results, we hypothesized that the inhibition of CXCL10 and RANTES secretion by SMC depended on Th1 cytokines. To test this hypothesis, we stimulated cultured SMC with different doses of IFN- $\gamma$  and measured the synthesis of CXCL10 and RANTES mRNA. Results show that the genetic expression of these chemokines was increased in response to IFN- $\gamma$  stimulation in a dose-dependent manner (Fig. 6D). Of note, the PI3K $\gamma$  inhibitor did not modify IFN- $\gamma$ -induced CXCL10 or RANTES synthesis even at high doses, excluding the involvement of SMC PI3K $\gamma$  (Fig. 6E). Altogether, these data indicate that PI3K $\gamma$  activity has an

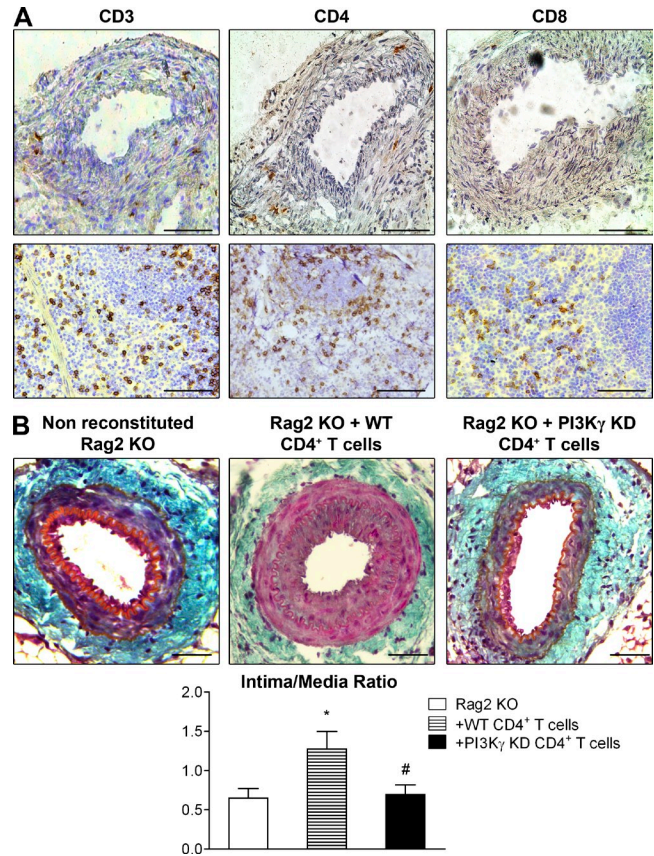


**Figure 5. PI3K $\gamma$  lipid kinase activity drives CD4<sup>+</sup> T cell-induced IH.** (A) Femoral arteries from WT mice were mechanically injured and immunostained for CD3, CD4, and CD8a. Consecutive representative photomicrographs show femoral artery and spleen sections with CD3 staining showing T cell content, CD4 staining showing CD4<sup>+</sup> T cell content, and CD8a staining showing CD8<sup>+</sup> T cells. (B) Rag2 KO recipient mice were reconstituted or not with CD4<sup>+</sup> T lymphocytes from WT or PI3K $\gamma$  KD donors. 2 d later, the femoral arteries of mice were mechanically injured and then analyzed 28 d after injury. Representative sections show injured femoral arteries stained with Masson Trichrome and histogram shows quantitative analysis of the intima/media ratio of indicated mice. Bars, 100  $\mu$ m. Data are expressed as mean  $\pm$  SEM and are representative of two independent experiments.  $n = 12$ –15 mice per group. \*,  $P < 0.05$  versus Rag2 KO; #,  $P < 0.05$  versus Rag2 KO + WT CD4<sup>+</sup> T cells. Data were analyzed with Mann-Whitney test.

impact on CXCL10 and RANTES secretion by SMC through modulation of IFN- $\gamma$  secretion.

#### Short-term inhibition of PI3K $\gamma$ protects against trauma induced by vascular injury in mouse and rat IH models

To validate the possibility of a PI3K $\gamma$  inhibitor being used for the prevention of restenosis, we evaluated the efficiency of a selective PI3K $\gamma$  inhibitor in two models of IH induction in rodents. Mice and rats were submitted to a short period of treatment with the PI3K $\gamma$ -selective inhibitor AS-605240 at a dose of 10 mg/kg/d for 2 d before and for the first 10 d after surgery (Fig. 7A).

28 d after mechanical injury of the femoral artery lesion, mice treated with AS-605240 showed a dramatic decrease (43% reduction) in the intima/media ratio compared with

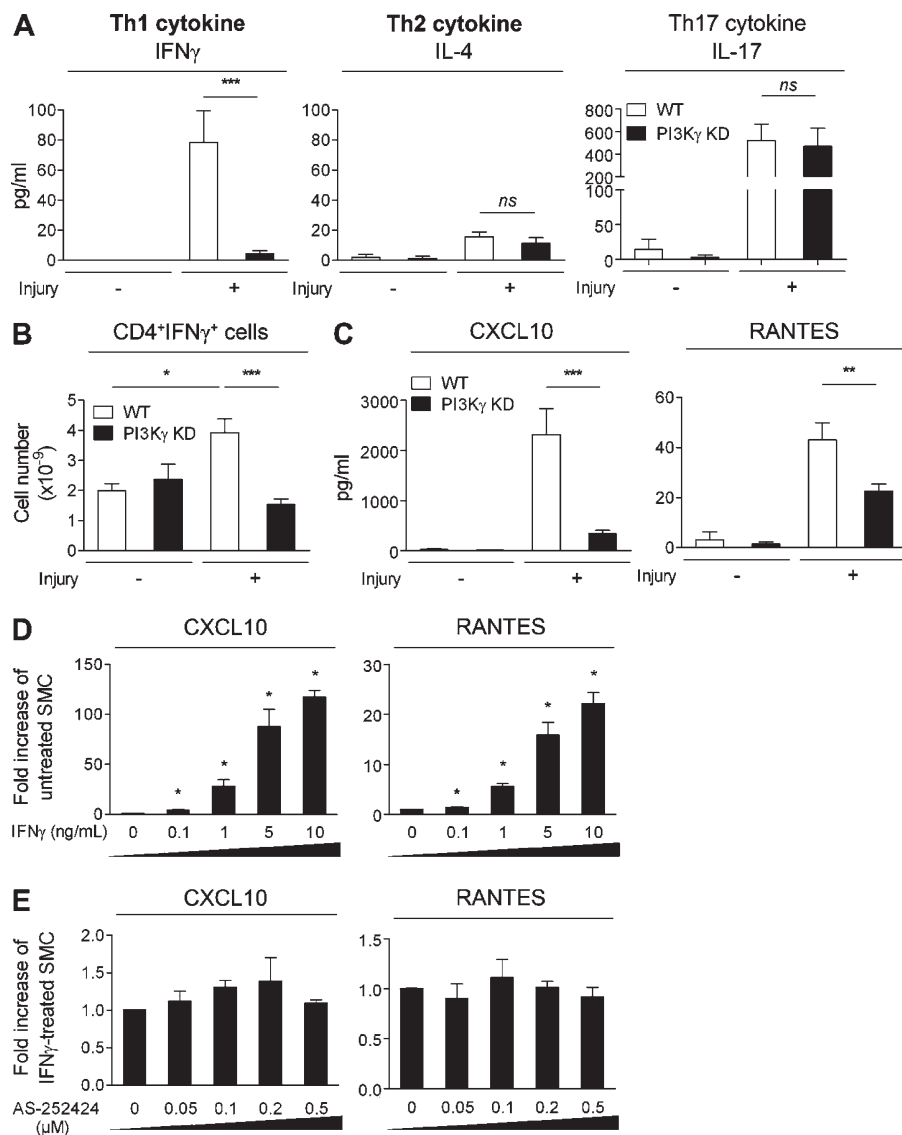


**Figure 6. Absence of PI3K $\gamma$  activity leads to a decreased SMC inflammatory response through Th1 cytokine modulation.** (A) WT and PI3K $\gamma$  KD femoral arteries were mechanically injured. 15 d later, arteries were harvested and cultured ex vivo in the presence of a PMA/Ionomycin cocktail. Levels of Th1, Th2, and Th17 cytokines were measured using Luminex technology in uninjured and injured arteries from WT and PI3K $\gamma$  KD mice. (B) WT and PI3K $\gamma$  KD femoral arteries were mechanically injured. 10 d later, inguinal lymph nodes (ILNs) were harvested and cells were immunostained for surface marker CD4 and intracellular content of IFN- $\gamma$ . Graphs represent the flow cytometry quantification of double-positive CD4<sup>+</sup>IFN $\gamma$ <sup>+</sup> cells. (C) WT and PI3K $\gamma$  KD femoral arteries were mechanically injured. 15 d later, arteries were harvested and cultured ex vivo in the presence of a PMA/Ionomycin cocktail. Levels of CXCL10 and RANTES were measured using Luminex technology in uninjured and injured arteries from WT and PI3K $\gamma$  KD mice. (D and E) CXCL10 and RANTES mRNA production was measured in cultured rat SMC treated with IFN- $\gamma$  for 48 h in a dose-dependent manner (D) or treated with 1 ng/ml IFN- $\gamma$  in the absence or presence of the PI3K $\gamma$ -specific inhibitor AS-252424 (E) at different doses (50, 100, 200, and 500 nM). Data are expressed as mean  $\pm$  SEM and are representative of two independent experiments,  $n = 10$  mice per group, for A, B, and C; and of three independent experiments for D and E. \*,  $P < 0.05$ ; \*\*,  $P < 0.01$ ; \*\*\*,  $P < 0.001$ ; ns, nonsignificant. Data were analyzed with Mann-Whitney test.

placebo-treated mice (Fig. 7 B). The level of inhibition caused by the treatment was comparable to that obtained in PI3K $\gamma$  KD mice, indicating that a short period of PI3K $\gamma$  inactivation was sufficient to decrease IH formation. Moreover, AS-605240 treatment did not induce additional inhibition of IH in PI3K $\gamma$  KD mice (Fig. 7 C), indicating that the observed effects were specifically due to PI3K $\gamma$  inhibition. To firmly establish the therapeutic benefit of PI3K $\gamma$  inhibition, we then used a rat carotid balloon injury model. 14 d after balloon injury, rats treated with AS-605240 showed a 59% reduction in the intima/media ratio compared with placebo-treated animals (Fig. 7 D). Altogether, these data demonstrate that a short period of PI3K $\gamma$  inhibition is sufficient to protect against IH in two different rodent models.

## DISCUSSION

In contrast to class IA PI3Ks that are ubiquitously expressed, PI3K $\gamma$  acts via G protein-coupled receptor signaling and presents an original expression profile. PI3K $\gamma$  is expressed by

hematopoietic cells and, albeit to a lesser extent, by cells of the cardiovascular system. Thus this kinase is an interesting protein in the field of cardiovascular disease research. Our previous work has identified PI3K $\gamma$  as an essential player in arterial wall inflammatory processes during atherosclerosis (Fougerat et al., 2008) and in SMC migration in vitro (Fougerat et al., 2012). In the present study, we have evaluated the suitability of PI3K $\gamma$  as a target for therapeutic intervention in the prevention of vascular damage after angioplasty. For this study, we used the femoral artery endovascular injury model that is characterized by neointima formation as a consequence of an excessive accumulation of SMC and deposition of extracellular matrix in the intimal layer of the vessel wall, a response which reflects the “in-stent” restenosis observed in humans (Lindner et al., 1993; Roque et al., 2000). Using this model, we show that pharmacological inhibition of PI3K $\gamma$ , genetic deletion of PI3K $\gamma$ , or expression of catalytically inactive PI3K $\gamma$  all lead

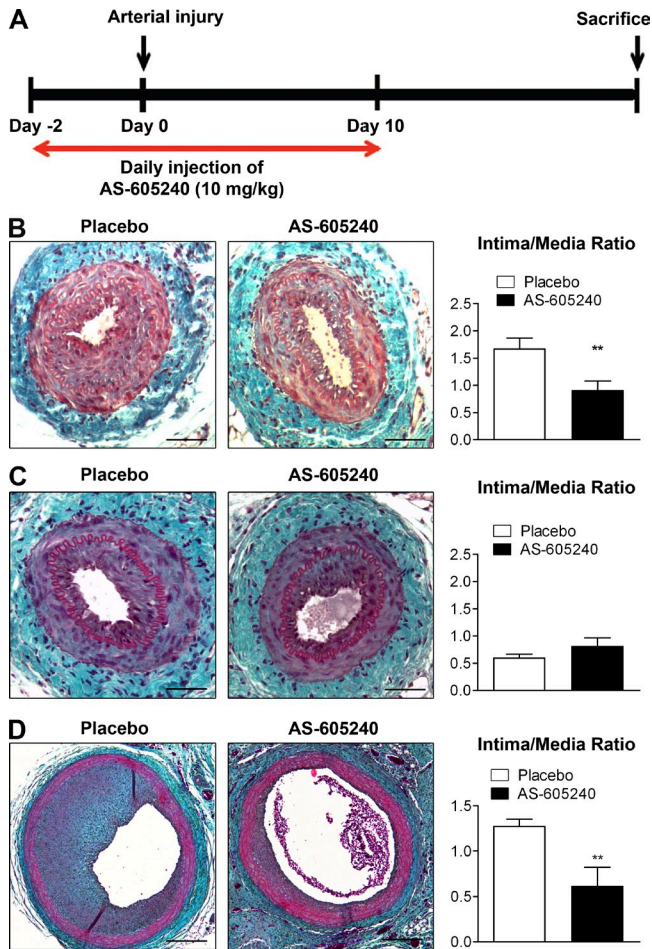


**Figure 7. A short-term pharmacological inhibition of PI3K $\gamma$  is sufficient to prevent IH.** (A) Schematic representation of the experimental protocol used to pharmacologically inactivate PI3K $\gamma$  in mouse and rat models of IH. Animals were injected daily with vehicle or the selective PI3K $\gamma$  inhibitor AS-605240 (10 mg/kg) from 2 d before until 10 d after arterial injury. At day 0, mice underwent femoral artery mechanical injury, whereas rats were submitted to carotid artery balloon injury. Histological analysis of injured artery cross sections was performed 28 d after injury in mice, and 14 d after injury in rats. (B) Representative cross sections show femoral arteries of placebo or AS-605240-treated WT mice stained with Masson Trichrome. Histogram shows quantitative analysis of the intima/media ratio in indicated mice. (C) Representative cross sections show femoral arteries of placebo- or AS-605240-treated PI3K $\gamma$  KD mice stained with Masson Trichrome. Histogram shows quantitative analysis of the intima/media ratio in indicated mice. (D) Representative cross sections show carotid arteries of placebo or AS-605240 treated Sprague Dawley (SD) rats stained with Masson Trichrome. Histogram shows quantitative analysis of the intima/media ratio in indicated rats. Bars: (B and C) 100  $\mu$ m; (D) 400  $\mu$ m. Data are expressed as mean  $\pm$  SEM and are representative of two independent experiments,  $n = 7$ –10 mice per group, for B and C; and of one experiment,  $n = 8$  rats per group, for D. \*\*,  $P < 0.01$ . Data were analyzed with a Mann-Whitney test.

to a dramatic decrease in IH without any modification of medial thickness. These data indicate that PI3K $\gamma$  activity is not involved in arterial remodeling but plays a role in neointima formation. To evaluate endothelial coverage in this model, we performed

an immunostaining of endothelial cells in injured arteries of mice from different genotypes. In the literature, little quantitative data is currently available about reendothelialization rate after mechanical femoral artery injury in the mouse (Tanaka et al., 2008). Here, we show with anti-CD31 staining 28 d after mechanical injury an incomplete endothelial coverage in WT mouse. Interestingly, reendothelialization seems improved in the absence of PI3K $\gamma$  or its activity. These data indicate that disruption of PI3K $\gamma$  activity leads to a decrease of IH without interfering with a correct reendothelialization. Nevertheless, additional investigation, including a quantitative approach of reendothelialization, needs to be done to better characterize the impact of absence of PI3K $\gamma$  in arterial healing.

Several lines of evidence strongly support a role for inflammation in the initiation of IH, and different inflammatory biomarkers have been linked to its progression. For example, regulation of NF- $\kappa$ B, a transcription factor involved in the production of many inflammatory immune mediators, induces a decrease in IH that is associated with reduced IL-6 expression (Niida et al., 2012). Reducing IL-1 $\beta$  levels by inhibiting its maturation in a pig model of in-stent restenosis also decreases neointimal size (Gyöngyösi et al., 2003). Moreover, suppression of TNF and IFN- $\gamma$  in a synergistic manner in the BM attenuates IH (Murayama et al., 2008). Consistent with these data, we found a strong up-regulation of mRNAs encoding IL-6, TNF, and IL-1 $\beta$  very early after lesion induction. Interestingly, mRNA synthesis of these cytokines was inhibited by 65% in the absence of PI3K $\gamma$  activity, suggesting a function for PI3K $\gamma$  in acute inflammatory processes. The use of chimeric mice that specifically express PI3K $\gamma$  in hematopoietic cells demonstrates that its activity in immune cells alone is sufficient to induce IH. The sequential recruitment of immune cells after vascular injury is still ill-defined. Roque et al. (2000) identified neutrophils adhering to the luminal side within 24 h after mechanical femoral artery injury. Boehm et al. (2004) reported the presence of macrophages both 1 and 2 wk after endovascular mechanical injury in periaortic tissue. They observed T lymphocytes in this area at the same time points. Our study provides new information on both the timing and the cell types involved in the development of IH. We have found that over the first 3 d after injury, monocytes/macrophages are the predominant cells present around the vessel. Then, T lymphocytes progressively accumulate in the periaortic tissue and can be detected at day 28. The exact function of T cells in the development of IH is controversial in the literature. Whereas Boehm et al. (2004) and Kovacic et al. (2010) reported that T cells are involved in the inflammatory processes of injured arterial walls leading to IH, Dimayuga et al. (2011) demonstrated that lymphocytes were protective against IH. This discrepancy regarding the role of T cells in vascular injury remains unclear, but perhaps the choice of injury model could explain the differences observed. Boehm et al. (2004) used an endovascular model of injury, whereas the other studies used a perivascular injury model, which involves placing a cuff around the artery. In agreement with this, a study performed by Tanaka et al. (2003)



clearly pinpointed the dominance of BM cell recruitment to the media and neointima after mechanical injury of the femoral artery when compared with cuff placement or ligation. The endovascular model would appear to be a better model for studying restenosis, as it is well established that lesions induced by bare metal stents are responsible for the first inflammatory events leading to IH (Toutouzas et al., 2004). The same discrepancy is found regarding the role of T cells in IH induced in the rat. Hansson et al. (1991) demonstrated that *mmu/mmu* rats developed more IH, indicating that T cells inhibit IH in rats. In contrast, there is some evidence suggesting a deleterious function of T cells in IH induced in the rat (George et al., 2001; Yoshimura et al., 2001). In the mouse, CD4<sup>+</sup> and CD8<sup>+</sup> T cells subpopulations seem to play opposite roles: CD4<sup>+</sup> T cells seem to play a deleterious effect in a model of periadventitial injury (Dimayuga et al., 2013), whereas CD8<sup>+</sup> T cells protect from IH formation (Dimayuga et al., 2013). Thus, it is possible that the apparent discrepancy observed in rat models could be related to a functional difference between CD4<sup>+</sup> and CD8<sup>+</sup> T cell subsets in IH development.

In our model, reconstitution of Rag2 KO mice with WT T cells restored the development of the disease, whereas PI3K $\gamma$  KD T cells did not, clearly indicating a role for T cells in IH and the importance of PI3K $\gamma$  in this cell type. The role of PI3K $\gamma$  in the maturation of thymocytes has been well studied, but its function in T cells has not yet been clearly established (Rodríguez-Borlado et al., 2003). In vitro data have shown that the absence of PI3K $\gamma$  leads to decreased IL-2 and IFN- $\gamma$  secretion in T cells stimulated by anti-CD3 antibodies, suggesting a role for PI3K $\gamma$  in Th1 polarization (Sasaki et al., 2000); however, in vivo data from a model of colitis induced by dextran sodium sulfate indicated that cytokines reflecting Th1 polarization are increased (van Dop et al., 2010). In a model of antigen-induced rheumatoid arthritis, Gruen et al. (2010) did not observe modifications in the production of Th1, Th2, or Th17 cytokines that could be dependent on PI3K $\gamma$ . The role of PI3K $\gamma$  in Th polarization is difficult to investigate, mostly because the number of T cells at the lesion site is modified in the absence of the kinase. One of the most important findings of our study is illustrated by the fact that the absence of PI3K $\gamma$  activity in T cells is sufficient to prevent IH despite a normal recruitment of immune cells (in Rag2 KO mice reconstituted with PI3K $\gamma$  KD T cells), clearly demonstrating a functional role for PI3K $\gamma$  in T cells in the development of the disease. Analysis of the cytokines present in injured arteries allowed us to identify a predominant Th1/Th17 phenotype, illustrated by high levels of IFN- $\gamma$  and IL-17 and little IL-4. IL-17 is produced at high levels in injured artery explants in the presence as well as in the absence of PI3K $\gamma$  activity, indicating that cells expressing IL-17 infiltrate injured arteries during IH development independently of PI3K $\gamma$ . Moreover, these results indicated that PI3K $\gamma$  was not involved in the Th17 responses after vascular injury. In contrast, IFN- $\gamma$  production was strongly inhibited in the absence of PI3K $\gamma$  activity, highlighting the importance of Th1 cells in IH. Moreover, analysis of intracytoplasmic production of

IFN- $\gamma$  in CD4<sup>+</sup> T cells collected from ILNs confirms the specific involvement of PI3K $\gamma$  in Th1 response. Surprisingly, we did not observe any difference concerning the IL-17 production by CD4<sup>+</sup> T cells originating from injured mice compared with uninjured mice. This contrasts with our results in injured arteries and suggest that a population other than CD4<sup>+</sup> T cells is responsible for IL-17 secretion. In this regard, IL-17-producing cells other than CD4<sup>+</sup> T cells have been described such as CD8<sup>+</sup>  $\alpha\beta$  T cells (Kondo et al., 2009),  $\gamma\delta$  T cells (O'Brien et al., 2009), LTI-like innate lymphoid cells (Takatori et al., 2009), NKT cells (Rachitskaya et al., 2008), CD3<sup>+</sup> invariant natural killer cells (Michel et al., 2007), and B cells (Schlegel et al., 2013). In addition, it is now widely accepted that diverse innate myeloid immune cells, such as monocytes and macrophages (Fujino et al., 2003), neutrophils (Hoshino et al., 2008), and mast cells (Lin et al., 2011), can produce IL-17. Regarding the number of monocytes/macrophages accumulated in the adventitia after arterial injury, we cannot exclude the possibility that, in injured arteries, these cells are able to secrete IL-17. Further experiments need to be done to better investigate the cell type involved in IL-17 secretion after arterial lesion. Together, these data are in agreement with our observation showing that PI3K $\gamma$  inhibition specifically modifies the Th1 T cell response in IH.

In the literature, the role of IFN- $\gamma$  on SMC proliferation is controversial. Wang et al. (2007) demonstrated that increased expression of IFN- $\gamma$ -induced SMC proliferation and intimal expansion in mouse. In contrast, Hansson and Holm (1991) and Castronuovo et al. (1995) demonstrated that injection of IFN- $\gamma$  into rat decreased IH after balloon injury. All of these studies used a model overexpressing IFN- $\gamma$  (by adenovirus or directly by injection of IFN- $\gamma$ ). We believe that the discrepancy between these findings could be due to the dose of IFN- $\gamma$  effectively received by the SMC. Indeed, there are several pieces of evidence demonstrating that, depending on the dose, IFN- $\gamma$  can activate or inhibit smooth cell proliferation (Shimokado et al., 1994). Using the inverse approach, Murayama et al. (2008) demonstrated that suppression of TNF and IFN- $\gamma$  in a synergistic manner in the BM attenuated IH, suggesting that endogenous IFN- $\gamma$  is involved in IH development. Interestingly, the transcriptomic analysis of atherectomy specimens and blood cells of patients with restenosis have been analyzed and indicated that IFN- $\gamma$  signaling is activated in neointimal SMC (Zohlh fer et al., 2001), suggesting a common involvement of Th1 cells in human restenosis.

Few studies have reported the role of Th17 cells in IH. IL-17 and IFN- $\gamma$  are produced concomitantly by human coronary infiltrating T cells during atherogenesis and act synergistically on vascular SMC to induce proinflammatory mediators such as CXCL10 and RANTES secretion (Eid et al., 2009). Our hypothesis was that similar mechanisms could exist after vascular injury and that PI3K $\gamma$ , by modulating IFN- $\gamma$  and not IL-17, could participate in the modulation of the SMC response. We then investigated CXCL10 and RANTES secretion in injured arteries and found that both of these chemokines are highly expressed in injured arteries, whereas

their levels are dramatically decreased in the absence of PI3K $\gamma$  activity. Moreover, our in vitro experiments showed that the PI3K $\gamma$  inhibitor did not modulate CXCL10 and RANTES mRNA synthesis by SMC, indicating that this kinase was not directly involved in the proinflammatory responses inherent to SMC. A deleterious role of RANTES in the modulation of inflammatory processes after arterial injury has already been described (Kovacic et al., 2010), whereas the role of CXCL10 is not well defined. CXCL10, also known as IFN- $\gamma$ -induced protein (IP-10), is involved in CXCR3-positive leukocyte recruitment in atheromas (Mach et al., 1999; Panzer et al., 2006; Proost et al., 2006; Vargas-Inchaustegui et al., 2010). Likewise, blockade or depletion of CXCR3 severely attenuates the recruitment of T cells to the site of inflammation at the arterial wall during the early stages of atherogenesis (Xie et al., 2003; Okamoto et al., 2008). Interestingly, an increase in CXCL10 secretion has been observed in patients with coronary artery disease who had undergone percutaneous transluminal coronary angioplasty and developed restenosis (Kawamura et al., 2003). Finally, interference with CXCL10 in a model of atherosclerosis injury led to a lower intima/media ratio than in a control group, strongly supporting a role for CXCL10 in IH (Zuojun et al., 2012). Nevertheless, the exact function of CXCL10 in arterial injuries is not fully understood. Our observation provides a strong argument in favor of a role for CXCL10 in IH and identifies a novel function for PI3K $\gamma$  in these processes. In this study, we cannot exclude the possibility of an additional source of IFN- $\gamma$  other than T cells during IH development. Indeed, Tenger et al. (2005) demonstrated that IFN- $\gamma$  can be produced by macrophages, NK cells, and vascular cells under the stimulation of IL-18 in the absence of T cells during atherogenesis. A recent paper indicated that the plasma levels of IL-18 correlated with the incidence of in-stent restenosis after percutaneous coronary intervention (Liu et al., 2013), but the exact function of IL-18 in IH development after vascular injury has not yet been evaluated. Further investigation needs to be done to identify the possible role of PI3K $\gamma$  in IL-18 secretion and its role in IH progression.

To firmly establish PI3K $\gamma$  as a real therapeutic target, we used pharmacological studies to demonstrate that treatment with a PI3K $\gamma$  inhibitor, used at a low dose and for a short period, was sufficient to prevent IH induced by vascular trauma. These data were obtained in injured vessels in mice and confirmed in a rat carotid artery balloon injury model that has the advantages of being highly reproducible and of mimicking the overstretch vascular damage induced by angioplasty (Tulis, 2007). Thus, these data validate PI3K $\gamma$  inhibition as an effective treatment in interventional cardiology. DESs are currently coated with antiproliferative agents such as sirolimus (rapamycin) and paclitaxel. Sirolimus, an inhibitor of the mammalian target of rapamycin (mTOR), is an immunosuppressive agent with antiproliferative, antimigratory, and antiinflammatory properties, exerting its effect by modulating the expression of a large number of intracellular genes (Marx et al., 1995; Poon et al., 2002; Marx et al., 2011). Paclitaxel is a lipophilic molecule derived from the Pacific yew tree *Taxus*

*brevifolia* and belongs to the family of microtubule-interfering agents. It is capable of inhibiting cellular division and motility by affecting microtubule organization (Belotti et al., 1996; Giannakakou et al., 2001). The clinical introduction of DES has clearly demonstrated a positive effect on IH, but emerging medium- to long-term follow-up data have raised concerns about their safety (Daemen et al., 2007). These molecules both seem to exert their antiproliferative effects not only on SMC but also on endothelial cells, leading to increased rates of late-stent thrombosis in patients with DES (Parry et al., 2005; Daemen et al., 2007). Experimental studies have also demonstrated that reendothelialization is clearly attenuated in patients treated with DES compared with patients with nude bare metal stents (Lüscher et al., 2007). Moreover, a local delivery of paclitaxel in a perivascular injury model applied to mice prone to atherosclerosis has been associated with excessive apoptosis of vascular cells, accompanied by degradation of the internal elastic lamina (Pires et al., 2007). The identification and development of promising novel therapies is therefore of great medical interest. PI3K $\gamma$  is not ubiquitously expressed and presents an original pattern of expression, with a high level of expression in immune cells and a low level of expression in the cardiovascular system (Fougerat et al., 2009). Thus, its major functions in vivo are in immune modulation and PI3K $\gamma$  inhibitors are therefore immune modulators rather than having the immunosuppressive effects of drugs such as sirolimus. Our results indicate that PI3K $\gamma$  inhibition did not interfere with cell proliferation but instead was restricted to the modulation of immune responses, leading to decreased IH without interfering with arterial healing.

Altogether, our data indicate that PI3K $\gamma$  plays a major role in the initiation and progression of IH by participating in monocyte and T cell recruitment but also by specifically modulating Th1 cytokines that, in combination with Th17 cytokines, are responsible for SMC inflammatory phenotype and especially involved in CXCL10 and RANTES secretion, resulting in the disease progression. These results, added to the benefit of a pharmacological inhibitor of PI3K $\gamma$  in two rodent models, definitively place PI3K $\gamma$  as a potential candidate for the prevention of arterial damage in interventional cardiology.

## MATERIALS AND METHODS

**Animals.** PI3K $\gamma$ -deficient (PI3K $\gamma$  KO) mice and mice expressing a catalytically inactive form of PI3K $\gamma$ , PI3K $\gamma$  kinase-dead mice (PI3K $\gamma$  KD), were from a C57BL/6J background and have been described earlier (Hirsch et al., 2000; Patrucco et al., 2004; Fougerat et al., 2008). Rag2 KO mice on a C57BL/6J background were from the breeding facility of PreCREFRE (UMS 06; Anexplo platform). WT, PI3K $\gamma$  KD, PI3K $\gamma$  KO, and Rag2 KO mice were maintained at the animal facility of Ranguel (UMS 06; Anexplo platform) and kept under SPF conditions. Sprague Dawley male rats weighing 400–450 g (Janvier SAS) were kept under SPF conditions at the animal facility UTE IRS-UN (Nantes, France). All animal procedures were conducted in accordance with institutional guidelines on Animal Experimentation and were under a French Ministry of Agriculture license.

**Femoral artery wire injury in mice.** WT, PI3K $\gamma$  KD, PI3K $\gamma$  KO, and Rag2 KO male mice aged 8–10 wk were investigated using an established model of femoral artery wire injury (Roque et al., 2000) for IH studies.

In brief, general anesthesia was achieved with 2% isoflurane. Then, the femoral artery was isolated and an incision was made under a surgical microscope (Carl Zeiss). A 0.35-mm diameter angioplasty guide wire with a 0.25-mm tip (gift from Abbott Vascular, Rungis, France) was advanced three times into the artery up to the level of the aortic bifurcation then pulled back. After removal of the wire, the arteriotomy site was ligated. Mice were sacrificed 6 h after the injury for RNA extraction and gene expression analysis, 15 d for ex vivo culture and cytokine production analysis, and 3, 8, or 28 d after the injury for histological and immunohistochemical analysis.

**Tissue processing and morphometry.** IH quantification was performed by the paraffin-embedment technique. At the point of euthanasia, mice were perfused with PBS, followed by 4% paraformaldehyde. Vessels were harvested and fixed in 4% formalin, pH = 8, for 24 h. They were put into paraffin and prepared as slides (4- $\mu$ m-thick sections). To quantify the rate of IH, sections were stained with Masson Trichrome, and then the lumen, IEL (internal elastic lamina), and EEL (external elastic lamina) perimeters ( $\mu$ m) were measured at 4 sections (0.5, 2.0, 3.5, and 5 mm from the ligation site) for each vessel using LAS software (Leica). Arteries that underwent an occlusive thrombotic event were excluded from the quantification group. The area defined by the EEL ( $\mu$ m<sup>2</sup>) was calculated assuming circular geometry in vivo: ( $A_{EEL} = EEL \text{ circumference}^2 \div 4\pi$ ). The area defined by the IEL ( $\mu$ m<sup>2</sup>) was calculated using: ( $A_{IEL} = IEL \text{ circumference}^2 \div 4\pi$ ). The lumen area ( $\mu$ m<sup>2</sup>) was calculated using: ( $A_{LUM} = Lumen \text{ circumference}^2 \div 4\pi$ ). The neointimal area ( $\mu$ m<sup>2</sup>) was calculated using: ( $A_{NEO} = A_{IEL} - A_{LUM}$ ). The medial area ( $\mu$ m<sup>2</sup>) was calculated using: ( $A_{MED} = A_{EEL} - A_{IEL}$ ). The intima/media ratio was calculated using: ( $neointima/media = A_{NEO} \div A_{MED}$ ).

**Immunohistochemistry.** For  $\alpha$ SM-actin, CD31, CD3, and F4/80 detection, vessels were embedded in paraffin. For CD3, CD4, and CD8 cell detection (Fig. 6 A), vessels were frozen with OCT compound and prepared as slides (5- $\mu$ m-thick sections). For all antigens except CD31, immunohistochemistry was performed using an ABC immunoperoxidase protocol. For CD31 detection, an immunofluorescence protocol was used. Primary antibodies for paraffin slide immunostaining were used to detect  $\alpha$ SM-actin-positive SMCs (actin, smooth muscle, rabbit polyclonal antibody, 1:25; Thermo Fisher Scientific), CD31 (PECAM-1)-positive endothelial cells (rat anti-mouse PECAM-1, 1:100; CliniSciences), T lymphocytes (rat anti-human CD3, 1:200; AbD Serotec), and macrophages (rat anti-mouse F4/80 antigen, 1/100; AbD Serotec). Primary antibodies for frozen section immunostaining were used to detect total T lymphocytes (clone SP7; Zymotend Systems), CD4 T cell subsets (anti-mouse CD4 purified, 1:10; eBioscience), and CD8 T cell subsets (anti-mouse CD8a purified, 1:100; eBioscience). All images were acquired using a microscope at 320 $\times$  (Leica).

**BM transplantation.** BM was obtained from 8-wk-old WT and PI3K $\gamma$  KD mice. BM cells were flushed from femurs and tibias then washed, filtered, counted, and resuspended in sterile PBS for retro-orbital injection of  $10^7$  unfractionated cells per WT or PI3K $\gamma$  KD irradiated mouse (9 Gy). 4 wk later, femoral artery injury was performed and mice were euthanized 28 d after the surgery. The successful engraftment was confirmed by PCR.

**Isolation of SMC from murine aorta and culture.** Mouse SMCs were isolated from WT mice according to a modified protocol described by Ray et al. (2001). In brief, aortae from 4 WT mice were dissected from their origin to the iliac bifurcation, flushed with PBS, and removed. The adventitia was removed from the aortae and the smooth tubes were cut into pieces of 1–2 mm, and then digested in 0.3% collagenase solution. Collagenase digestion was stopped by adding DMEM/10% FBS (FBS). Then, the pieces of aortae were washed twice and seeded in culture dishes coated with 10  $\mu$ g/ml human fibronectin (BD). Primary confluent cultures were trypsinized (0.1% trypsin; Thermo Fisher Scientific) at 37°C, and then cells were incubated at 37°C in 5% CO<sub>2</sub> in DMEM/10% FBS and cultured until the fourth passage.

**Measure of mouse SMC proliferation.** Primary mouse SMCs were subcultured onto 24-well cell culture plates at a seeding density of  $2.5 \times 10^4$

cells/well. The wells were washed twice with PBS and placed into serum-free medium containing 0.2% BSA or 10% FBS in the presence or absence of increased concentrations of the PI3K $\gamma$ -specific inhibitor AS-242525 (Sigma-Aldrich) for 72 h. Then, SMC proliferation was measured by using a XTT cell proliferation assay kit (Roche).

**Gene expression analysis in injured arteries.** At the point of euthanasia, mice were perfused with ice-cold sterile PBS into the heart. The two injured femoral arteries were collected into TRIzol reagent and stored at  $-20^\circ\text{C}$ . Samples were automatically homogenized using a FastPrep-24 instrument (MP Biomedicals). To extract RNA, chloroform was added to the samples. After centrifugation, the aqueous phase was collected and isopropanol was added to precipitate the RNA. The RNA pellet was washed and resuspended in RNase-free water. 1  $\mu$ g RNA was reverse transcribed using random hexamer primers (Invitrogen). IL-6 (forward primer: 5'-GAGGATACCACTCCCAA-CAGACC-3', reverse primer: 5'-AAGTGCATCATCGTTGTTTCATACA-3'), IL-1 $\beta$  (forward primer: 5'-GGAGTTTGAGTCTGCAGAGTTCCC-3', reverse primer: 5'-ACAGGCTTGTGCTCTGCTTGTG-3'), and TNF (forward primer: 5'-CATCTTCTCAAATTCGAGTGACAA-3', reverse primer: 5'-TGGGAGTAGACAAGGTACAACCC-3') expression was analyzed by real-time quantitative PCR by means of SyBR Green Light-Cycler480 technology (Roche). The Rps29 gene was used as a reference and gene expression quantification was performed using the classic  $2^{-\Delta\Delta C_t}$  method. Results were expressed as fold increase over the uninjured control.

**CD3<sup>+</sup> and CD4<sup>+</sup> T cell isolation and transplantation.** CD3<sup>+</sup> or CD4<sup>+</sup> cells were isolated from WT and PI3K $\gamma$  KD mice by negative selection using a Pan T cell isolation kit II (Miltenyi Biotec) or CD4<sup>+</sup> T Cell Isolation kit II (Miltenyi Biotec), according to the manufacturer's instructions. The purity of the isolated fraction was confirmed by FACS analysis for CD3<sup>+</sup> or CD4<sup>+</sup> T cells using anti-CD3 $\epsilon$ -PE or CD4-FITC antibodies (Miltenyi Biotec).  $10^7$  cells of each type per mouse were injected into Rag2 KO mice retro-orbitally 2 d before femoral artery wire injury. Mice were euthanized 28 d later. Their successful reconstitution with T lymphocytes was confirmed by FACS analysis on the sacrifice date.

**Cytokine measurements in ex vivo cultured femoral arteries.** WT and PI3K $\gamma$  KD mice were submitted ( $n = 14$  per group) or not ( $n = 6$  per group) to mechanical femoral artery injury. 15 d after injury, mice were sacrificed. Arteries were harvested and cut into 3-mm-long rings. Rings were cultured in DMEM supplemented with 10% FBS and 1% penicillin-streptomycin (complete medium) for 4 h. Then, the medium was replaced with complete medium with added PMA (1  $\mu$ g/ml) and ionomycin (1  $\mu$ g/ml) to stimulate cytokine release. 3 d later, the supernatants were collected. Cytokine levels in the supernatants were measured according to the immunoassay protocol for MILLIPLEX Map Mouse Cytokine/Chemokine Magnetic Bead Panel kit (Millipore) on the Luminex 100 system at the "Phenotypage" service (Anexplo platform). Cytokine levels were determined in pg/ml compared with a standard range.

**Intracellular cytokine staining and flow cytometry analysis in ILNs.** WT and PI3K $\gamma$  KD mice were submitted or not to mechanical femoral artery injury. 10 d after injury, mice were sacrificed. ILNs were harvested and dissociated. Cells from ILNs were stimulated with 0.1  $\mu$ g/ml PMA, 1  $\mu$ g/ml ionomycin, and 1  $\mu$ g/ml monensin at 37°C, in a humidified 5% CO<sub>2</sub> atmosphere for 4 h. After staining of the surface markers, 1  $\mu$ g/ml TCR (PerCP-Cy5.5 hamster anti-mouse TCR- $\beta$  chain; BD) and 1  $\mu$ g/ml CD4 (Alexa Fluor 700 rat anti-mouse CD4; BD), cells were fixed and permeabilized with Cytofix/Cytoperm and Perm/Wash buffer (e-Bioscience) according to manufacturer's instructions. Cells were then incubated with antibodies against 1  $\mu$ g/ml IFN- $\gamma$  (APC rat anti-mouse IFN- $\gamma$ ; BD), and 1  $\mu$ g/ml IL-17A (Alexa Fluor 488 rat anti-mouse IL-17A; BD) or isotype controls for 20 min, and washed twice with Perm/Wash buffer before flow cytometry analysis (LSR-Fortessa; BD).



**SMC culture and IFN- $\gamma$  treatment.** Rat aortic SMC (A7r5 clonal cell line; American Type Culture Collection) were grown in DMEM supplemented with 10% FCS and 1% penicillin/streptomycin, at 37°C in 5% CO<sub>2</sub>, and used at passages 2 to 12. SMCs were serum-starved before treatment with recombinant rat IFN- $\gamma$  in the presence or absence of AS-252424 (Sigma-Aldrich) for 48 h.

**Gene expression analysis in SMC.** Rat aortic SMCs were incubated with indicated concentrations of IFN- $\gamma$  during 48 h, and then washed with PBS and collected in TRIZOL reagent (Life Technologies) to quantify CXCL10 and RANTES mRNA expression. RNA extraction, reverse transcription, and CXCL10 (forward primer: 5'-TGTCGCATGTTGAGAT-CATTGC-3'; reverse primer: 5'-TCCGGATTACAGACACCTCTTCTC-3') and RANTES (forward primer: 5'-AAGTGCTCCAACCTTGCAGTC-GTC-3'; reverse primer: 5'-CTTCTTCTCTGGGTTGGCACACAC-3') expression were analyzed as described above for mouse femoral arteries. The rat Rpl13 gene was used as a reference. The results were expressed as fold increase of control condition in absence of FBS or IFN- $\gamma$ .

**Treatment with PI3K $\gamma$  inhibitor.** A pharmacological inhibitor of PI3K $\gamma$ , AS-605240 (Cayman Chemical), was intraperitoneally administered (10 mg/kg/d) to WT mice, PI3K $\gamma$  KD mice, or Sprague-Dawley rats. All animals were pretreated with the PI3K $\gamma$  inhibitor from 2 d before until 10 d after femoral artery mechanical injury for mice and carotid artery balloon injury for rats.

**Rat carotid artery balloon injury.** A total of 16 male 10-month-old Sprague-Dawley rats weighing 400 to 450 g (Janvier SAS) were used in this study. The balloon denudation injuries were performed in rat carotid arteries after the procedure previously described (Tulis, 2007). In brief, rats were anesthetized with 2% isoflurane. A midline incision was made in the neck to expose the left external carotid artery. A 2F Fogarty balloon catheter (Edwards Lifesciences) was introduced into the left external carotid artery and advanced through the common carotid artery to the aortic arch. The balloon was inflated at 3 atm with a medical inflation device (Medtronic), resulting in a 5-mm-long injury. This procedure was repeated two more times (a total of three passes), and then the catheter was removed. The external carotid was ligated, and the incision was sutured. 14 d later, arteries were harvested, flushed with PBS, and fixed with 4% formalin. They were put into paraffin and prepared as slides (4- $\mu$ m-thick sections). The sections were stained with Masson Trichrome and the quantification was made at 4 sections for each artery (1, 2, 3, and 4 mm from the proximal injury site) using LAS software. Intimal and medial areas were measured and calculated in the same manner as in the mouse injury model.

**Statistical analysis.** All results are presented as means  $\pm$  SEM. Comparisons between groups were made using the Mann-Whitney test for independent samples. Outcomes of  $P < 0.05$  were considered to be significant. Analyses were performed using Prism 5 (GraphPad Software).

We thank the technical service of the animal facilities, the NON-INVASIVE exploration service for use of their irradiator, the Phenotype Analysis Facility, and the histopathology service (US006/CREFRE INSERM/UPS, Toulouse). We thank the GeT Platform (genomics and transcriptomics) of Toulouse Genopole (I2MC/UMR1048). We thank the IBISA platform Cardiex (Nantes) for functional explorations in rats. We are grateful to Cécile Allières (INSERM U1034, PESSAC) for her technical help.

This work was supported by the Midi-Pyrénées Region, the French Foundation, and the National Research Agency (ANR-JCJC). S. Gayral was supported by the Foundation for Medical Research (FRM) and the Lefoulon-Delalande foundation.

The authors declare no competing financial interests.

Submitted: 19 June 2013

Accepted: 19 June 2014

## REFERENCES

- Alcázar, I., M. Marqués, A. Kumar, E. Hirsch, M. Wymann, A.C. Carrera, and D.F. Barber. 2007. Phosphoinositide 3-kinase  $\gamma$  participates in T cell receptor-induced T cell activation. *J. Exp. Med.* 204:2977–2987. <http://dx.doi.org/10.1084/jem.20070366>
- Belotti, D., M. Rieppi, M.I. Nicoletti, A.M. Casazza, T. Fojo, G. Tarabozzi, and R. Giavazzi. 1996. Paclitaxel (Taxol(R)) inhibits motility of paclitaxel-resistant human ovarian carcinoma cells. *Clin. Cancer Res.* 2:1725–1730.
- Bennett, M.R. 2003. In-stent stenosis: pathology and implications for the development of drug eluting stents. *Heart.* 89:218–224. <http://dx.doi.org/10.1136/heart.89.2.218>
- Bikkina, M., and J. Koneru. 2011. Long-term effectiveness and safety of sirolimus drug-eluting stents. *Med Devices (Auckl).* 4:117–124. <http://dx.doi.org/10.2147/MDER.S11749>
- Boehm, M., M. Olive, A.L. True, M.F. Crook, H. San, X. Qu, and E.G. Nabel. 2004. Bone marrow-derived immune cells regulate vascular disease through a p27(Kip1)-dependent mechanism. *J. Clin. Invest.* 114:419–426. <http://dx.doi.org/10.1172/JCI200420176>
- Castronuovo, J.J. Jr., S.B. Guss, D. Mysh, A. Sawhney, M. Wolff, and A.M. Gown. 1995. Cytokine therapy for arterial restenosis: inhibition of neointimal hyperplasia by gamma-interferon. *Cardiovasc. Surg.* 3:463–468. [http://dx.doi.org/10.1016/0967-2109\(95\)94442-Y](http://dx.doi.org/10.1016/0967-2109(95)94442-Y)
- Costa, M.A., and D.I. Simon. 2005. Molecular basis of restenosis and drug-eluting stents. *Circulation.* 111:2257–2273. <http://dx.doi.org/10.1161/01.CIR.0000163587.36485.A7>
- Daemen, J., P. Wenaweser, K. Tsuchida, L. Abrecht, S. Vaina, C. Morger, N. Kukreja, P. Jüni, G. Sianos, G. Hellge, et al. 2007. Early and late coronary stent thrombosis of sirolimus-eluting and paclitaxel-eluting stents in routine clinical practice: data from a large two-institutional cohort study. *Lancet.* 369:667–678. [http://dx.doi.org/10.1016/S0140-6736\(07\)60314-6](http://dx.doi.org/10.1016/S0140-6736(07)60314-6)
- Dangas, G.D., B.E. Claessen, A. Caixeta, E.A. Sanidas, G.S. Mintz, and R. Mehran. 2010. In-stent restenosis in the drug-eluting stent era. *J. Am. Coll. Cardiol.* 56:1897–1907. <http://dx.doi.org/10.1016/j.jacc.2010.07.028>
- Dimayuga, P.C., K.Y. Chyu, J. Kirzner, J. Yano, X. Zhao, J. Zhou, P.K. Shah, and B. Cercek. 2011. Enhanced neointima formation following arterial injury in immune deficient Rag-1<sup>-/-</sup> mice is attenuated by adoptive transfer of CD8<sup>+</sup> T cells. *PLoS ONE.* 6:e20214. <http://dx.doi.org/10.1371/journal.pone.0020214>
- Dimayuga, P.C., K.Y. Chyu, W.M. Lio, X. Zhao, J. Yano, J. Zhou, T. Honjo, P.K. Shah, and B. Cercek. 2013. Reduced neointima formation after arterial injury in CD4<sup>-/-</sup> mice is mediated by CD8<sup>+</sup>CD28<sup>hi</sup> T cells. *J. Am. Heart Assoc.* 2:e000155. <http://dx.doi.org/10.1161/JAHA.113.000155>
- Dzau, V.J. 2003. Predicting the future of human gene therapy for cardiovascular diseases: what will the management of coronary artery disease be like in 2005 and 2010? *Am. J. Cardiol.* 92:32N–35N. [http://dx.doi.org/10.1016/S0002-9149\(03\)00966-4](http://dx.doi.org/10.1016/S0002-9149(03)00966-4)
- Eid, R.E., D.A. Rao, J. Zhou, S.F. Lo, H. Ranjbaran, A. Gallo, S.I. Sokol, S. Pfau, J.S. Pober, and G. Tellides. 2009. Interleukin-17 and interferon- $\gamma$  are produced concomitantly by human coronary artery-infiltrating T cells and act synergistically on vascular smooth muscle cells. *Circulation.* 119:1424–1432. <http://dx.doi.org/10.1161/CIRCULATIONAHA.108.827618>
- Farb, A., D.K. Weber, F.D. Kolodgie, A.P. Burke, and R. Virmani. 2002. Morphological predictors of restenosis after coronary stenting in humans. *Circulation.* 105:2974–2980. <http://dx.doi.org/10.1161/01.CIR.0000019071.72887.BD>
- Fougerat, A., S. Gayral, P. Gourdy, A. Schambourg, T. Rückle, M.K. Schwarz, C. Rommel, E. Hirsch, J.F. Arnal, J.P. Salles, et al. 2008. Genetic and pharmacological targeting of phosphoinositide 3-kinase- $\gamma$  reduces atherosclerosis and favors plaque stability by modulating inflammatory processes. *Circulation.* 117:1310–1317. <http://dx.doi.org/10.1161/CIRCULATIONAHA.107.720466>
- Fougerat, A., S. Gayral, N. Malet, F. Briand-Mesange, M. Breton-Douillon, and M. Laffargue. 2009. Phosphoinositide 3-kinases and their role in inflammation: potential clinical targets in atherosclerosis? *Clin. Sci.* 116:791–804. <http://dx.doi.org/10.1042/CS20080549>
- Fougerat, A., N.F. Smirnova, S. Gayral, N. Malet, E. Hirsch, M.P. Wymann, B. Perret, L.O. Martinez, M. Douillon, and M. Laffargue. 2012. Key role of PI3K $\gamma$  in monocyte chemotactic protein-1-mediated amplification of PDGF-induced aortic smooth muscle cell migration.

- Br. J. Pharmacol. 166:1643–1653. <http://dx.doi.org/10.1111/j.1476-5381.2012.01866.x>
- Fujino, S., A. Andoh, S. Bamba, A. Ogawa, K. Hata, Y. Araki, T. Bamba, and Y. Fujiyama. 2003. Increased expression of interleukin 17 in inflammatory bowel disease. *Gut*. 52:65–70. <http://dx.doi.org/10.1136/gut.52.1.65>
- George, J., S. Greenberg, I. Barshack, M. Singh, S. Pri-Chen, S. Laniado, and G. Keren. 2001. Accelerated intimal thickening in carotid arteries of balloon-injured rats after immunization against heat shock protein 70. *J. Am. Coll. Cardiol.* 38:1564–1569. [http://dx.doi.org/10.1016/S0735-1097\(01\)01579-0](http://dx.doi.org/10.1016/S0735-1097(01)01579-0)
- Giannakakou, P., R. Robey, T. Fojo, and M.V. Blagosklonny. 2001. Low concentrations of paclitaxel induce cell type-dependent p53, p21 and G1/G2 arrest instead of mitotic arrest: molecular determinants of paclitaxel-induced cytotoxicity. *Oncogene*. 20:3806–3813. <http://dx.doi.org/10.1038/sj.onc.1204487>
- Grassia, G., M. Maddaluno, A. Guglielmotti, G. Mangano, G. Biondi, P. Maffia, and A. Ialenti. 2009. The anti-inflammatory agent bindarit inhibits neointima formation in both rats and hyperlipidaemic mice. *Cardiovasc. Res.* 84:485–493. <http://dx.doi.org/10.1093/cvr/cvp238>
- Gruen, M., C. Rose, C. König, M. Gajda, R. Wetzker, and R. Bräuer. 2010. Loss of phosphoinositide 3-kinase  $\gamma$  decreases migration and activation of phagocytes but not T cell activation in antigen-induced arthritis. *BMC Musculoskelet. Disord.* 11:63. <http://dx.doi.org/10.1186/1471-2474-11-63>
- Gyöngyösi, M., W. Sperker, C. Csonka, D. Bonderman, I. Lang, C. Strehblow, C. Adlbrecht, M. Shirazi, U. Windberger, S. Marlovits, et al. 2003. Inhibition of interleukin-1 $\beta$  convertase is associated with decrease of neointimal hyperplasia after coronary artery stenting in pigs. *Mol. Cell. Biochem.* 249:39–43. <http://dx.doi.org/10.1023/A:1024701715131>
- Hansson, G.K., and J. Holm. 1991. Interferon-gamma inhibits arterial stenosis after injury. *Circulation*. 84:1266–1272. <http://dx.doi.org/10.1161/01.CIR.84.3.1266>
- Hansson, G.K., J. Holm, S. Holm, Z. Fotev, H.J. Hedrich, and J. Fingerle. 1991. T lymphocytes inhibit the vascular response to injury. *Proc. Natl. Acad. Sci. USA*. 88:10530–10534. <http://dx.doi.org/10.1073/pnas.88.23.10530>
- Hirsch, E., V.L. Katanaev, C. Garlanda, O. Azzolino, L. Pirola, L. Silengo, S. Sozzani, A. Mantovani, F. Altruda, and M.P. Wymann. 2000. Central role for G protein-coupled phosphoinositide 3-kinase  $\gamma$  in inflammation. *Science*. 287:1049–1053. <http://dx.doi.org/10.1126/science.287.5455.1049>
- Horvath, C., F.G. Welt, M. Nedelman, P. Rao, and C. Rogers. 2002. Targeting CCR2 or CD18 inhibits experimental in-stent restenosis in primates: inhibitory potential depends on type of injury and leukocytes targeted. *Circ. Res.* 90:488–494. <http://dx.doi.org/10.1161/hh0402.105956>
- Hoshino, A., T. Nagao, N. Nagi-Miura, N. Ohno, M. Yasuhara, K. Yamamoto, T. Nakayama, and K. Suzuki. 2008. MPO-ANCA induces IL-17 production by activated neutrophils in vitro via FC region- and complement-dependent manner. *J. Autoimmun.* 31:79–89. <http://dx.doi.org/10.1016/j.jaut.2008.03.006>
- Kawamura, A., S. Miura, M. Fujino, H. Nishikawa, Y. Matsuo, H. Tanigawa, S. Tomita, Y. Tsuchiya, K. Matsuo, and K. Saku. 2003. CXCR3 chemokine receptor-plasma IP10 interaction in patients with coronary artery disease. *Circ. J.* 67:851–854. <http://dx.doi.org/10.1253/circj.67.851>
- Kondo, T., H. Takata, F. Matsuki, and M. Takiguchi. 2009. Cutting edge: Phenotypic characterization and differentiation of human CD8<sup>+</sup> T cells producing IL-17. *J. Immunol.* 182:1794–1798. <http://dx.doi.org/10.4049/jimmunol.0801347>
- Kovacic, J.C., R. Gupta, A.C. Lee, M. Ma, F. Fang, C.N. Tolbert, A.D. Walts, L.E. Beltran, H. San, G. Chen, et al. 2010. Stat3-dependent acute Rantes production in vascular smooth muscle cells modulates inflammation following arterial injury in mice. *J. Clin. Invest.* 120:303–314. <http://dx.doi.org/10.1172/JCI40364>
- Laffargue, M., R. Calvez, P. Finan, A. Trifilieff, M. Barbier, F. Altruda, E. Hirsch, and M.P. Wymann. 2002. Phosphoinositide 3-kinase gamma is an essential amplifier of mast cell function. *Immunity*. 16:441–451. [http://dx.doi.org/10.1016/S1074-7613\(02\)00282-0](http://dx.doi.org/10.1016/S1074-7613(02)00282-0)
- Lagerqvist, B., S.K. James, U. Stenestrand, J. Lindbäck, T. Nilsson, and L. Wallentin. SCAAR Study Group. 2007. Long-term outcomes with drug-eluting stents versus bare-metal stents in Sweden. *N. Engl. J. Med.* 356:1009–1019. <http://dx.doi.org/10.1056/NEJMoa067722>
- Lin, A.M., C.J. Rubin, R. Khandpur, J.Y. Wang, M. Riblett, S. Yalavarthi, E.C. Villanueva, P. Shah, M.J. Kaplan, and A.T. Bruce. 2011. Mast cells and neutrophils release IL-17 through extracellular trap formation in psoriasis. *J. Immunol.* 187:490–500. <http://dx.doi.org/10.4049/jimmunol.1100123>
- Lindner, V., J. Fingerle, and M.A. Reidy. 1993. Mouse model of arterial injury. *Circ. Res.* 73:792–796. <http://dx.doi.org/10.1161/01.RES.73.5.792>
- Liu, W., Y. Liu, H. Jiang, X. Ding, R. Zhu, B. Li, and Y. Zhao. 2013. Plasma levels of interleukin 18, interleukin 10, and matrix metalloproteinase-9 and -137G/C polymorphism of interleukin 18 are associated with incidence of in-stent restenosis after percutaneous coronary intervention. *Inflammation*. 36:1129–1135. <http://dx.doi.org/10.1007/s10753-013-9647-6>
- Lüscher, T.F., J. Steffel, F.R. Eberli, M. Joner, G. Nakazawa, F.C. Tanner, and R. Virmani. 2007. Drug-eluting stent and coronary thrombosis: biological mechanisms and clinical implications. *Circulation*. 115:1051–1058. <http://dx.doi.org/10.1161/CIRCULATIONAHA.106.675934>
- Mach, F., A. Sauty, A.S. Iarossi, G.K. Sukhova, K. Neote, P. Libby, and A.D. Luster. 1999. Differential expression of three T lymphocyte-activating CXC chemokines by human atheroma-associated cells. *J. Clin. Invest.* 104:1041–1050. <http://dx.doi.org/10.1172/JCI6993>
- Marx, S.O., T. Jayaraman, L.O. Go, and A.R. Marks. 1995. Rapamycin-FKBP inhibits cell cycle regulators of proliferation in vascular smooth muscle cells. *Circ. Res.* 76:412–417. <http://dx.doi.org/10.1161/01.RES.76.3.412>
- Marx, S.O., H. Totary-Jain, and A.R. Marks. 2011. Vascular smooth muscle cell proliferation in restenosis. *Circ. Cardiovasc. Interv.* 4:104–111. <http://dx.doi.org/10.1161/CIRCINTERVENTIONS.110.957332>
- Michel, M.L., A.C. Keller, C. Paget, M. Fujio, F. Trottein, P.B. Savage, C.H. Wong, E. Schneider, M. Dy, and M.C. Leite-de-Moraes. 2007. Identification of an IL-17-producing NK1.1<sup>neg</sup> iNKT cell population involved in airway neutrophilia. *J. Exp. Med.* 204:995–1001. <http://dx.doi.org/10.1084/jem.20061551>
- Murayama, H., M. Takahashi, M. Takamoto, Y. Shiba, H. Ise, J. Koyama, Y. Tagawa, Y. Iwakura, and U. Ikeda. 2008. Deficiency of tumour necrosis factor- $\alpha$  and interferon- $\gamma$  in bone marrow cells synergistically inhibits neointimal formation following vascular injury. *Cardiovasc. Res.* 80:175–180. <http://dx.doi.org/10.1093/cvr/cvn250>
- Niida, T., K. Isoda, M. Kitagaki, N. Ishigami, T. Adachi, O. Matsubara, K. Takeda, T. Kishimoto, and F. Ohsuzu. 2012. I $\kappa$ BNS regulates interleukin-6 production and inhibits neointimal formation after vascular injury in mice. *Cardiovasc. Res.* 93:371–379. <http://dx.doi.org/10.1093/cvr/cvr323>
- O'Brien, R.L., C.L. Roark, and W.K. Born. 2009. IL-17-producing  $\gamma\delta$  T cells. *Eur. J. Immunol.* 39:662–666. <http://dx.doi.org/10.1002/eji.200839120>
- Okamoto, Y., E.J. Folco, M. Minami, A.K. Wara, M.W. Feinberg, G.K. Sukhova, R.A. Colvin, S. Kihara, T. Funahashi, A.D. Luster, and P. Libby. 2008. Adiponectin inhibits the production of CXC receptor 3 chemokine ligands in macrophages and reduces T-lymphocyte recruitment in atherosclerosis. *Circ. Res.* 102:218–225. <http://dx.doi.org/10.1161/CIRCRESAHA.107.164988>
- Panzer, U., O.M. Steinmetz, R.R. Reinking, T.N. Meyer, S. Fehr, A. Schneider, G. Zahner, G. Wolf, U. Helmchen, P. Schaerli, et al. 2006. Compartment-specific expression and function of the chemokine IP-10/CXCL10 in a model of renal endothelial microvascular injury. *J. Am. Soc. Nephrol.* 17:454–464. <http://dx.doi.org/10.1681/ASN.2005040364>
- Parry, T.J., R. Brosius, R. Thyagarajan, D. Carter, D. Argentieri, R. Falotico, and J. Siekierka. 2005. Drug-eluting stents: sirolimus and paclitaxel differentially affect cultured cells and injured arteries. *Eur. J. Pharmacol.* 524:19–29. <http://dx.doi.org/10.1016/j.ejphar.2005.09.042>
- Patrucco, E., A. Notte, L. Barberis, G. Selvetella, A. Maffei, M. Brancaccio, S. Marengo, G. Russo, O. Azzolino, S.D. Rybalkin, et al. 2004. PI3K $\gamma$  modulates the cardiac response to chronic pressure overload by distinct kinase-dependent and -independent effects. *Cell*. 118:375–387. <http://dx.doi.org/10.1016/j.cell.2004.07.017>
- Perino, A., A. Ghigo, E. Ferrero, F. Morello, G. Santulli, G.S. Baillie, F. Damilano, A.J. Dunlop, C. Pawson, R. Walser, et al. 2011. Integrating cardiac PIP3 and cAMP signaling through a PKA anchoring function of p110 $\gamma$ . *Mol. Cell*. 42:84–95. <http://dx.doi.org/10.1016/j.molcel.2011.01.030>
- Pires, N.M., D. Eeffing, M.R. de Vries, P.H. Quax, and J.W. Jukema. 2007. Sirolimus and paclitaxel provoke different vascular pathological responses after local delivery in a murine model for restenosis on underlying atherosclerotic arteries. *Heart*. 93:922–927. <http://dx.doi.org/10.1136/hrt.2006.102244>

- Poon, M., J.J. Badimon, and V. Fuster. 2002. Overcoming restenosis with sirolimus: from alphabet soup to clinical reality. *Lancet*. 359:619–622. [http://dx.doi.org/10.1016/S0140-6736\(02\)07751-6](http://dx.doi.org/10.1016/S0140-6736(02)07751-6)
- Proost, P., S. Struyf, T. Loos, M. Gouwy, E. Schutyser, R. Conings, I. Ronsse, M. Parmentier, B. Grillet, G. Opdenakker, et al. 2006. Coexpression and interaction of CXCL10 and CD26 in mesenchymal cells by synergising inflammatory cytokines: CXCL8 and CXCL10 are discriminative markers for autoimmune arthropathies. *Arthritis Res. Ther.* 8:R107. <http://dx.doi.org/10.1186/ar1997>
- Rachitskaya, A.V., A.M. Hansen, R. Horai, Z. Li, R. Villasmil, D. Luger, R.B. Nussenblatt, and R.R. Caspi. 2008. Cutting edge: NKT cells constitutively express IL-23 receptor and ROR $\gamma$ t and rapidly produce IL-17 upon receptor ligation in an IL-6-independent fashion. *J. Immunol.* 180:5167–5171. <http://dx.doi.org/10.4049/jimmunol.180.8.5167>
- Ray, J.L., R. Leach, J.M. Herbert, and M. Benson. 2001. Isolation of vascular smooth muscle cells from a single murine aorta. *Methods Cell Sci.* 23:185–188. <http://dx.doi.org/10.1023/A:1016357510143>
- Rodríguez-Borlado, L., D.F. Barber, C. Hernández, M.A. Rodríguez-Marcos, A. Sánchez, E. Hirsch, M. Wymann, C. Martínez-A, and A.C. Carrera. 2003. Phosphatidylinositol 3-kinase regulates the CD4/CD8 T cell differentiation ratio. *J. Immunol.* 170:4475–4482. <http://dx.doi.org/10.4049/jimmunol.170.9.4475>
- Roque, M., J.T. Fallon, J.J. Badimon, W.X. Zhang, M.B. Taubman, and E.D. Reis. 2000. Mouse model of femoral artery denudation injury associated with the rapid accumulation of adhesion molecules on the luminal surface and recruitment of neutrophils. *Arterioscler. Thromb. Vasc. Biol.* 20:335–342. <http://dx.doi.org/10.1161/01.ATV.20.2.335>
- Sasaki, T., J. Irie-Sasaki, R.G. Jones, A.J. Oliveira-dos-Santos, W.L. Stanford, B. Bolon, A. Wakeham, A. Itie, D. Bouchard, I. Kozieradzki, et al. 2000. Function of PI3K $\gamma$  in thymocyte development, T cell activation, and neutrophil migration. *Science*. 287:1040–1046. <http://dx.doi.org/10.1126/science.287.5455.1040>
- Schlegel, P.M., I. Steiert, I. Kötter, and C.A. Müller. 2013. B cells contribute to heterogeneity of IL-17 producing cells in rheumatoid arthritis and healthy controls. *PLoS ONE*. 8:e82580. <http://dx.doi.org/10.1371/journal.pone.0082580>
- Schwartz, R.S., E.J. Topol, P.W. Serruys, G. Sangiorgi, and D.R. Holmes Jr. 1998. Artery size, neointima, and remodeling: time for some standards. *J. Am. Coll. Cardiol.* 32:2087–2094.
- Shimokado, K., T. Yokota, N. Kato, C. Kosaka, T. Sasaguri, J. Masuda, J. Ogata, and F. Numano. 1994. Bidirectional regulation of smooth muscle cell proliferation by IFN- $\gamma$ . *J. Atheroscler. Thromb.* 1:S29–S33. [http://dx.doi.org/10.5551/jat1994.1.Supp1\\_S29](http://dx.doi.org/10.5551/jat1994.1.Supp1_S29)
- Takatori, H., Y. Kanno, W.T. Watford, C.M. Tato, G. Weiss, I.I. Ivanov, D.R. Littman, and J.J. O’Shea. 2009. Lymphoid tissue inducer-like cells are an innate source of IL-17 and IL-22. *J. Exp. Med.* 206:35–41. <http://dx.doi.org/10.1084/jem.20072713>
- Tanaka, K., M. Sata, Y. Hirata, and R. Nagai. 2003. Diverse contribution of bone marrow cells to neointimal hyperplasia after mechanical vascular injuries. *Circ. Res.* 93:783–790. <http://dx.doi.org/10.1161/01.RES.0000096651.13001.B4>
- Tanaka, K., M. Sata, T. Natori, J.R. Kim-Kaneyama, K. Nose, M. Shibamura, Y. Hirata, and R. Nagai. 2008. Circulating progenitor cells contribute to neointimal formation in nonirradiated chimeric mice. *FASEB J.* 22:428–436. <http://dx.doi.org/10.1096/fj.06-6884com>
- Tenger, C., A. Sundborger, J. Jawien, and X. Zhou. 2005. IL-18 accelerates atherosclerosis accompanied by elevation of IFN- $\gamma$  and CXCL16 expression independently of T cells. *Arterioscler. Thromb. Vasc. Biol.* 25:791–796. <http://dx.doi.org/10.1161/01.ATV.0000153516.02782.65>
- Toutouzas, K., A. Colombo, and C. Stefanadis. 2004. Inflammation and restenosis after percutaneous coronary interventions. *Eur. Heart J.* 25:1679–1687. <http://dx.doi.org/10.1016/j.ehj.2004.06.011>
- Tulis, D.A. 2007. Rat carotid artery balloon injury model. *Methods Mol. Med.* 139:1–30. [http://dx.doi.org/10.1007/978-1-59745-571-8\\_1](http://dx.doi.org/10.1007/978-1-59745-571-8_1)
- van Dop, W.A., S. Marengo, A.A. te Velde, E. Ciraolo, I. Franco, F.J. ten Kate, G.E. Boeckxstaens, J.C. Hardwick, D.W. Hommes, E. Hirsch, and G.R. van den Brink. 2010. The absence of functional PI3K $\gamma$  prevents leukocyte recruitment and ameliorates DSS-induced colitis in mice. *Immunol. Lett.* 131:33–39. <http://dx.doi.org/10.1016/j.imlet.2010.03.008>
- Vargas-Inchaustegui, D.A., A.E. Hogg, G. Tulliano, A. Llanos-Cuentas, J. Arevalo, J.J. Endsley, and L. Soong. 2010. CXCL10 production by human monocytes in response to *Leishmania braziliensis* infection. *Infect. Immun.* 78:301–308. <http://dx.doi.org/10.1128/IAI.00959-09>
- Wang, Y., Y. Bai, L. Qin, P. Zhang, T. Yi, S.A. Teesdale, L. Zhao, J.S. Pober, and G. Tellides. 2007. Interferon- $\gamma$  induces human vascular smooth muscle cell proliferation and intimal expansion by phosphatidylinositol 3-kinase dependent mammalian target of rapamycin raptor complex 1 activation. *Circ. Res.* 101:560–569. <http://dx.doi.org/10.1161/CIRCRESAHA.107.151068>
- Xie, J.H., N. Nomura, M. Lu, S.L. Chen, G.E. Koch, Y. Weng, R. Rosa, J. Di Salvo, J. Mudgett, L.B. Peterson, et al. 2003. Antibody-mediated blockade of the CXCR3 chemokine receptor results in diminished recruitment of T helper 1 cells into sites of inflammation. *J. Leukoc. Biol.* 73:771–780. <http://dx.doi.org/10.1189/jlb.1102573>
- Yoshimura, S., R. Morishita, K. Hayashi, K. Yamamoto, H. Nakagami, Y. Kaneda, N. Sakai, and T. Ogihara. 2001. Inhibition of intimal hyperplasia after balloon injury in rat carotid artery model using cis-element ‘decoy’ of nuclear factor- $\kappa$ B binding site as a novel molecular strategy. *Gene Ther.* 8:1635–1642. <http://dx.doi.org/10.1038/sj.gt.3301566>
- Zohlhhofer, D., T. Richter, F. Neumann, T. Nührenberg, R. Wessely, R. Brandl, A. Murr, C.A. Klein, and P.A. Baeuerle. 2001. Transcriptome analysis reveals a role of interferon- $\gamma$  in human neointima formation. *Mol. Cell.* 7:1059–1069. [http://dx.doi.org/10.1016/S1097-2765\(01\)00239-8](http://dx.doi.org/10.1016/S1097-2765(01)00239-8)
- Zuojun, H., H. Lingyu, H. Wei, Y. Henghui, Z. Chonggang, W. Jingsong, W. Mian, L. Yong, and W. Shenming. 2012. Interference of IP-10 expression inhibits vascular smooth muscle cell proliferation and intimal hyperplasia in carotid artery: a new insight in the prevention of restenosis. *Cell Biochem. Biophys.* 62:125–135. <http://dx.doi.org/10.1007/s12013-011-9270-9>